

STABILITY ANALYSIS OF π -KINKS IN A $0-\pi$ JOSEPHSON JUNCTION*

G. DERKS[†], A. DOELMAN[‡], S.A. VAN GILS[§], AND H. SUSANTO[¶]

Abstract. We consider a spatially non-autonomous discrete sine-Gordon equation with constant forcing and its continuum limit(s) to model a $0-\pi$ Josephson junction with an applied bias current. The continuum limits correspond to the strong coupling limit of the discrete system. The non-autonomous character is due to the presence of a discontinuity point, namely a jump of π in the sine-Gordon phase. The continuum models admits static solitary waves which are called π -kinks and are attached to the discontinuity point. For small forcing, there are three types of π -kinks. We show that one of the kinks is stable and the others are unstable. There is a critical value of the forcing beyond all static π -kinks fail to exist. Up to this value, the (in)stability of the π -kinks can be established analytically in the strong coupling limits. Applying a forcing above the critical value causes the nucleation of 2π -kinks and -antikinks. Besides a π -kink, the unforced system also admits a static 3π -kink. This state is unstable in the continuum models. By combining analytical and numerical methods in the discrete model, it is shown that the stable π -kink remains stable, and that the unstable π -kinks cannot be stabilized by decreasing the coupling. The 3π -kink does become stable in the discrete model when the coupling is sufficiently weak.

Key words. $0-\pi$ Josephson junction, $0-\pi$ sine-Gordon equation, semifluxon, π -kink

AMS subject classifications. 34D35, 35Q53, 37K50, 39A11

1. Introduction. One important application of the sine-Gordon equation is to describe the propagation of magnetic flux (fluxons) in long Josephson junctions [18, 5]. The flux quanta or fluxons are described by the kinks of the sine-Gordon equation. When many small Josephson junctions are connected through the inductance of the superconductors, they form a discrete Josephson transmission line. The propagation of a fluxon is then described by the discrete sine-Gordon equation. For some materials, Josephson junctions are more easily fabricated in the form of a lattice than as a long continuous Josephson junction. In the strong coupling limit, a discrete Josephson junction lattice becomes a long Josephson junction.

It was proposed in the late 70's by Bulaevskii that a phase-shift of π may occur in the sine-Gordon equation due to magnetic impurities [7]. Only recently this prediction is confirmed experimentally [35]. Present technological advances can also impose a π -phase-shift in a long Josephson junction using, e.g., superconductors with unconventional pairing symmetry [34], Superconductor-Ferromagnet-Superconductor (SFS) π -junctions [29], or Superconductor-Normal metal-Superconductor (SNS) junctions in which the charge-carrier population in the conduction channels is controlled [4].

A junction containing a region with a phase jump of π is then called a $0-\pi$ Josephson junction and is described by a $0-\pi$ sine-Gordon equation. The place where the

*This work was supported by the Royal Netherlands Academy of Art and Sciences (KNAW) and Netherlands Organization for Scientific Research (NWO).

[†]Department of Mathematics, University of Surrey, Guildford, Surrey, GU2 7XH (g.derks@surrey.ac.uk),

[‡]Department 'Modelling, Analysis and Simulation', Center for Mathematics and Computer Science (CWI), Kruislaan 413, 1098 SJ Amsterdam, and Korteweg-de Vries Institute, Faculty of Sciences, University of Amsterdam, Plantage Muidergracht 24, 1018 TV Amsterdam, The Netherlands (a.doelman@cwi.nl),

[§]Department of Applied Mathematics, University of Twente, P.O. Box 217, 7500AE Enschede, The Netherlands (s.a.vangils@math.utwente.nl),

[¶]Department of Mathematics and Statistics, University of Massachusetts, Amherst MA 01003-4515, USA (susanto@math.umass.edu)

0-junction meets the π -junction is called a discontinuity point. A $0-\pi$ Josephson junction admits a half magnetic flux (semifluxon), sometimes called π -fluxon, attached to the discontinuity point [14]. A semifluxon is represented by a π -kink in the $0-\pi$ sine-Gordon equation [32].

Using the technology described in [14], a $0-\pi$ array of Josephson junctions can be created as well. Such system can be modeled by a discrete $0-\pi$ sine-Gordon equation. A short numerical study of a discrete π -kink is given in [31].

The presence of the semifluxon in a $0-\pi$ Josephson junction or a $0-\pi$ array of Josephson junctions opens a new field where many questions, that have been discussed in detail for the 2π -kink (fluxon) in the sine-Gordon equation, can be addressed for the π -kink too. The fact that the π -kink cannot move in space, even in the continuum case, will give a different qualitative behavior such as the disappearance of the zero eigenvalue (Goldstone mode), as will be shown later.

In this paper we will study both the continuous and discrete $0-\pi$ sine-Gordon equation, especially the stability of the kinks admitted by the equations. Knowing the eigenvalues of a kink is of interest for experimentalists, since the corresponding eigenfunctions (localized modes) can play an important role in the behavior of the kink [27].

The present work is organized as follows: in section 2 we will describe the mathematical model of the problem and its interpretation as a Josephson junction system. We will discuss the discrete system as well as several continuum approximations. In section 3 we consider the continuous $0-\pi$ sine-Gordon equation which describes a continuous long Josephson junction with discontinuity point. It is also the lowest order continuum approximation for the discrete system, not reflecting any lattice spacing (coupling) effects. In [32] it is shown that there exist three types of π -kinks in the $0-\pi$ sine-Gordon equation. We will analyze their stability and show that one type is stable and the other two are unstable. A higher order continuum approximation, which includes terms representing a small lattice spacing (strong coupling), is considered in section 4. It is shown that for small values of the lattice spacing parameter, the three types of π -kinks persist and their stability properties do not change. In section 5 the discrete $0-\pi$ sine-Gordon with large lattice spacing (small coupling) is analyzed, especially the existence and stability of π -kinks. Numerical calculations connecting the regions of small and large lattice spacing (weak and strong coupling) will be presented in section 6. In this section the analytical results of the previous sections are linked together. Conclusions and plans for future research are presented in section 7.

2. Mathematical models for $0-\pi$ junctions.

2.1. The discrete $0-\pi$ sine-Gordon equation. The Lagrangian describing the phase of a $0-\pi$ array of Josephson junctions is given by

$$(2.1) \quad L = \int \sum_{n \in \mathbb{Z}} \left[\frac{1}{2} \left(\frac{d\phi_n}{dt} \right)^2 - \frac{1}{2} \left(\frac{\phi_{n+1} - \phi_n}{a} \right)^2 - 1 + \cos(\phi_n + \theta_n) + \gamma \phi_n \right] dt,$$

where ϕ_n is the Josephson phase of the n th junction. The phase jump of π in the Josephson phase is described by θ_n where

$$(2.2) \quad \theta_n = \begin{cases} 0, & n \leq 0, \\ -\pi, & 0 < n. \end{cases}$$

The Lagrangian (2.1) is given in nondimensionalized form. The lattice spacing parameter a is normalized to the Josephson length λ_J , the time t is normalized to the

inverse plasma frequency ω_0^{-1} and the applied bias current density $\gamma > 0$ is scaled to the critical current density J_c .

The equation of the phase motion generated by the Lagrangian (2.1) is the discrete 0 - π sine-Gordon equation

$$(2.3) \quad \ddot{\phi}_n - \frac{\phi_{n-1} - 2\phi_n + \phi_{n+1}}{a^2} = -\sin(\phi_n + \theta_n) + \gamma.$$

We use $n \in \mathbb{Z}$ for the analytical calculations, but of course, the fabrication of the junction as well as the numerics are limited to a finite number of sites, say $2N$. We will take the boundary conditions to represent the way in which the applied magnetic field $h = H/(\lambda_J J_c)$ enters the system, i.e.,

$$(2.4) \quad \frac{\phi_{-N+1} - \phi_{-N}}{a} = \frac{\phi_N - \phi_{N-1}}{a} = h.$$

In the sequel we will always consider the case when there is no applied magnetic field, i.e., we will take $h = 0$.

2.2. Approximations to the lattice spacing in the continuum limit.

There are various continuum model approximations for (2.3) that can be derived in the continuum limit $a \ll 1$. Writing $\phi_n = \phi(na)$ and expanding the difference terms using a Taylor expansion gives

$$\frac{\phi_{n-1} - 2\phi_n + \phi_{n+1}}{a^2} = 2 \sum_{k=0}^{\infty} \frac{a^{2k}}{(2k+2)!} \partial_{xx}^k \phi_{xx}(na) = L_a \phi_{xx}$$

and

$$\frac{\phi_{n+1} - \phi_n}{a} = \sum_{k=0}^{\infty} \frac{a^k}{(k+1)!} \partial_x^k \phi(na) = \tilde{L}_a \phi_x.$$

Thus the continuum approximation for (2.3) is

$$(2.5) \quad \phi_{tt} - L_a \phi_{xx} = -\sin(\phi + \theta) + \gamma,$$

where $\theta(x)$ is defined similar to (2.2), i.e.,

$$\theta(x) = \begin{cases} 0, & x < 0, \\ -\pi, & x > 0. \end{cases}$$

The continuum approximation for the Lagrangian is

$$L = \iint_{-\infty}^{\infty} \left[\frac{1}{2} (\phi_t)^2 - \frac{1}{2} (\tilde{L}_a \phi_x)^2 - 1 + \cos(\phi + \theta) + \gamma \phi \right] dx dt$$

Note that the normalizations in the discrete system imply that the spatial coordinate x is normalized to the Josephson length λ_J .

There are several ways to derive approximations for the operator L_a when $a \rightarrow 0$, see for example [28]. The first obvious approximation is

$$(2.6) \quad \phi_{tt} - \phi_{xx} - \frac{a^2}{12} \phi_{xxxx} = -\sin(\phi + \theta) + \gamma, \quad x \neq 0.$$

Another approximation can be found by using that $(1 - \frac{a^2}{12}\partial_{xx})L_a = 1 - \frac{a^4}{240}\partial_{xx}^2 + \dots$. This results reflects the invertibility of L_a up to fourth order. Hence $(1 - \frac{a^2}{12}\partial_{xx})$ acting on (2.5) gives the approximation (up to fourth order terms)

$$(2.7) \quad \phi_{xx} = \phi_{tt} + \sin(\phi + \theta) - \gamma - \frac{a^2}{12}\partial_{xx}(\phi_{tt} + \sin(\phi + \theta)), \quad x \neq 0.$$

Expanding this equation and using the expression for ϕ_{xx} again, we get

$$(2.8) \quad \begin{aligned} \phi_{xx} &= \phi_{tt} + \sin(\phi + \theta) - \gamma \\ &\quad - \frac{a^2}{12}(\phi_{tttt} + [\sin(\phi + \theta)]_{tt} - \phi_x^2 \sin(\phi + \theta) \\ &\quad + \cos(\phi + \theta)[\phi_{tt} + \sin(\phi + \theta) - \gamma]), \quad x \neq 0. \end{aligned}$$

The steady state equation for (2.6) is

$$\phi_{xx} + \frac{a^2}{12}\phi_{xxxx} = \sin(\phi + \theta) - \gamma, \quad x \neq 0,$$

while (2.7) yields the equation

$$\phi_{xx} = (1 - \frac{a^2}{12}\partial_{xx})\sin(\phi + \theta) - \gamma, \quad x \neq 0,$$

and (2.8) gives

$$\phi_{xx} = \sin(\phi + \theta) - \gamma - \frac{a^2}{12}(-\phi_x^2 \sin(\phi + \theta) + \cos(\phi + \theta)[\sin(\phi + \theta) - \gamma]), \quad x \neq 0.$$

Unfortunately the last two equations are not Hamiltonian, so we have lost the Hamiltonian properties of the original system, while the first equation is singularly perturbed.

Yet another approximation that has a variational structure and is not singularly perturbed can be obtained by combining the two equations that have lost their variational character. Indeed, taking (2.7) twice and subtracting (2.8) gives

$$(2.9) \quad \begin{aligned} \phi_{xx} &= \phi_{tt} + \sin(\phi + \theta) - \gamma \\ &\quad - \frac{a^2}{12}(2\phi_{xxtt} + 2\phi_{xx} \cos(\phi + \theta) - \phi_x^2 \sin(\phi + \theta) - \phi_{ttt} - \phi_{tt} \cos(\phi + \theta) \\ &\quad + \phi_t^2 \sin(\phi + \theta) - \cos(\phi + \theta)(\phi_{tt} + \sin(\phi + \theta) - \gamma)), \quad x \neq 0. \end{aligned}$$

The Lagrangian for this system is

$$\begin{aligned} L &= \iint \left[\frac{1}{2}\phi_t^2 - \frac{1}{2}\phi_x^2 - 1 + \cos(\phi + \theta) + \gamma\phi \right. \\ &\quad \left. + \frac{a^2}{2} \left[\phi_x \partial_x (\phi_{tt} + \sin(\phi + \theta)) + \frac{1}{2}(\phi_{tt} + \sin(\phi + \theta) - \gamma)^2 \right] \right] dx dt. \end{aligned}$$

The static equation for (2.9) is

$$(2.10) \quad \begin{aligned} \phi_{xx} &= \sin(\phi + \theta) - \gamma \\ &\quad - \frac{a^2}{12}(2\phi_{xx} \cos(\phi + \theta) - \phi_x^2 \sin(\phi + \theta) - \cos(\phi + \theta)(\sin(\phi + \theta) - \gamma)), \quad x \neq 0. \end{aligned}$$

This equation is a regularly perturbed Hamiltonian system with the Hamiltonian

$$H(\phi, p) = \frac{p^2}{2(1 + \frac{a^2}{6} \cos(\phi + \theta))} + \gamma\phi + \cos(\phi + \theta) - \frac{a^2}{24} (\sin(\phi + \theta) - \gamma)^2,$$

which implies $p = \phi_x \left(1 + \frac{a^2 \cos(\phi + \theta)}{6}\right)$.

In this paper, we will analyze equation (2.9) as a continuum strong interaction limit which incorporates some effects of the lattice spacing into the model. The model equation (2.9) is chosen as it is non-singular and has the same conservative properties as the discrete system, reflecting its physical properties.

3. The π -kinks and their spectra in the continuum limit. In this section, we will consider (2.9) for $a = 0$, which is a model for an ideal long $0-\pi$ Josephson junction:

$$(3.1) \quad \phi_{tt} - \phi_{xx} + \sin(\phi + \theta) = \gamma, \quad x \neq 0.$$

For a Josephson junction without an applied bias current or a phase jump, i.e., for $\gamma = 0$ and $\theta(x) \equiv 0$, the model corresponds to the sine-Gordon equation. A stable solution of the sine-Gordon equation is the basic (normalized) stationary, monotonically increasing fluxon, given by

$$(3.2) \quad \phi_{\text{flux}}(x) = 4 \arctan e^x, \quad \phi_{\text{flux}}(0) = \pi$$

(see [10]).

In general the discontinuous function $\theta(x)$ in (3.1) will introduce a discontinuity at $x = 0$ for the second derivative ϕ_{xx} . Hence, the natural solution space for (3.1) consists of functions which are spatially continuous and have a continuous spatial derivative. The behavior at infinity is regulated by requiring that the spatial derivative of the solution belongs to $H_1(\mathbb{R})$ (which allows the phase to converge to a nonzero constant at infinity). Therefore, the equation (3.1) is considered as a dynamical system on the function space

$$\mathbb{H} = \{\phi : \mathbb{R} \rightarrow \mathbb{R} \mid \phi_x \in H_1(\mathbb{R})\}.$$

It is straightforward to find that for $|\gamma| < 1$ and $x < 0$, the “fixed points” of (3.1) are $\phi_s^- = \arcsin(\gamma)$ and $\phi_c^- = -\arcsin(\gamma) + \pi$. Similarly, for $|\gamma| < 1$ and $x > 0$, they are $\phi_s^+ = \arcsin(\gamma) + \pi$ and $\phi_c^+ = -\arcsin(\gamma) + 2\pi$. In [32], it is shown that there exists various types of stationary fronts, which connect the equilibria. Most stationary fronts are so-called π -kinks, which are static waves connecting equilibrium states at $x = \pm\infty$ with a phase-difference of π . Such waves are solutions of the static wave equation

$$(3.3) \quad \phi_{xx} - \sin(\phi + \theta) = -\gamma, \quad x \neq 0.$$

In the x -dynamics of (3.3), the points ϕ_s^\pm are saddle points and the points with ϕ_c^\pm are center points. Thus a π -kink connects ϕ_s^- with ϕ_s^+ .

In this section we will consider the stability of those π -kinks. For completeness, we first describe the various types of π -kinks as found in [32]. These π -kinks are constructed by taking suitable combinations of the phase portraits for $\theta = 0$ and $\theta = -\pi$. The phase portraits for $\gamma = 0$ are essentially different from the ones for $0 < \gamma < 1$ (the case $-1 < \gamma < 0$ follows from this one by taking $\phi \mapsto -\phi$ and

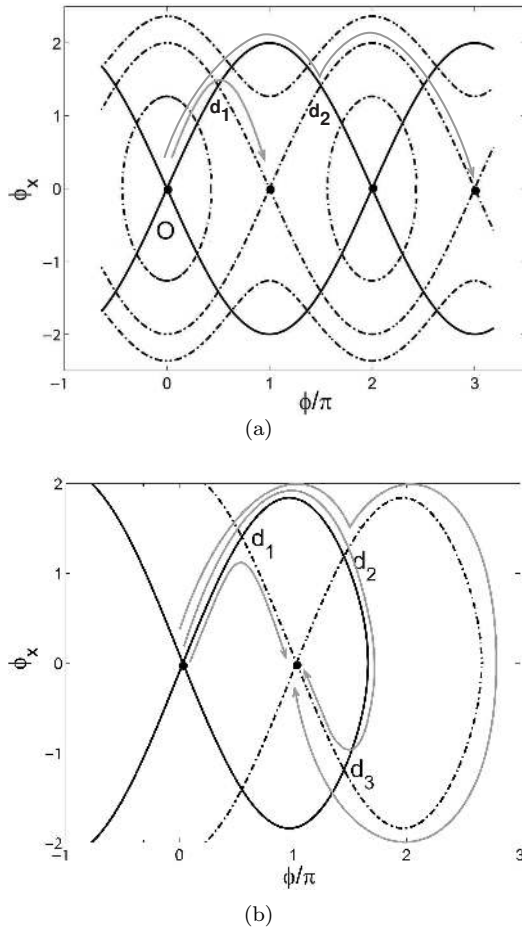


FIG. 3.1. (a) The phase portrait of system (3.3) for $\gamma = 0$. The trajectories for $x < 0$ are indicated with bold lines, the trajectories for $x > 0$ with dashed lines. Any orbit of (3.1) switches at $x = 0$ from bold to dashed. The type 1 semifluxon switches at d_1 and corresponds to one of the gray arrow-lines. The 3π -fluxon switches at d_2 and is denoted by the other gray arrow-line. (b) The phase portrait of system (3.3) for $\gamma = 0.1$. For simplicity, only the stable and unstable manifolds of the fixed points are shown. Apart from d_1 , there are also the points d_2 or d_3 which can be used for the switch position of $x = 0$ to obtain a solution with a phase difference π between the end points.

$\gamma \mapsto -\gamma$). In case $\gamma > 0$ there are homoclinic connections at $k\pi + \arcsin(\gamma)$, $k \in \mathbb{Z}$, k even ($\theta = 0$) or k odd ($\theta = -\pi$). If $\gamma = 0$, then these homoclinic connections break to heteroclinic connections between $k\pi$ and $(k+2)\pi$.

The phase portrait of (3.3) for $\gamma = 0$ is shown in Figure 3.1(a). Following the notation in [32], in case $\gamma = 0$, there are two types of heteroclinic connections (kinks) in the $0-\pi$ junction. The first one, called *type 1* and denoted by $\phi_\pi^1(x; 0)$, connects 0 and π . The point in the phase plane where the junction lies is denoted by $d_1(0)$. The second one, called *type 2* and denoted by $\phi_{3\pi}^2(x; 0)$, connects 0 and 3π . Now the point in the phase plane where the junction lies is denoted by $d_2(0)$. This solution is not a semifluxon, but it will play a role in the analysis of some of the semifluxons for $\gamma \neq 0$.

If $0 < \gamma \ll 1$, then there are three types of π -kinks (heteroclinic connections) in

the junction, all connecting $\arcsin(\gamma)$ and $\pi + \arcsin(\gamma)$. A phase portrait of (3.3) for nonzero γ is shown in Figure 3.1(b). The first semifluxon, called *type 1* and denoted by $\phi_\pi^1(x; \gamma)$, is a continuation of the connection at $\gamma = 0$. The point in the phase plane where the junction lies is denoted by $d_1(\gamma)$. The π -fluxon $\phi_\pi^1(x; \gamma)$ is monotonically increasing.

The second one is called *type 2* and denoted by $\phi_\pi^2(x; \gamma)$. In the limit for $\gamma \rightarrow 0$, it breaks in the 3π -kink and the heteroclinic connection between 3π and π (a -2π -kink or an anti-fluxon). The point in the phase plane where the junction lies is denoted by $d_2(\gamma)$. The π -fluxon $\phi_\pi^2(x; \gamma)$ is not monotonically increasing, but has a hump.

The third one is called *type 3* and denoted by $\phi_\pi^3(x; \gamma)$. In the limit for $\gamma \rightarrow 0$, it breaks in the heteroclinic connection between 0 and 2π (fluxon) and an anti-semifluxon like the type 1 wave but connecting 2π and π . The point in the phase plane where the junction lies is denoted by $d_3(\gamma)$. This π -fluxon has a hump too, but a lower one than the type 2 wave. Following the first homoclinic orbit, the junction points are ordered such that $d_1(\gamma)$ comes first, followed by $d_2(\gamma)$, followed by $d_3(\gamma)$ (see Figure 3.1(b)).

If γ increases, the points $d_2(\gamma)$ and $d_3(\gamma)$ approach each other, until they coincide at [32]

$$(3.4) \quad \gamma = \gamma^* = \frac{2}{\sqrt{4 + \pi^2}}$$

in the point $(\pi + \arcsin(\gamma^*), 0)$. At this point, the type 2 wave $\phi_\pi^2(x; \gamma)$ ceases to exist (in the limit it breaks into half the homoclinic connection for $x < 0$ and the full homoclinic connection for $x > 0$). The type 3 kink $\phi_\pi^3(x; \gamma^*)$ consists of half the homoclinic connection for $x < 0$ and the fixed point for $x > 0$ and this wave can be continued for $\gamma > \gamma^*$. For $\gamma > \gamma^*$, the type 3 kink is monotonic.

If γ increases further, the points $d_1(\gamma)$ and $d_3(\gamma)$ approach each other [32] until they coincide at

$$(3.5) \quad \gamma = \gamma_{\text{cr}} = \frac{2}{\pi}.$$

When $\gamma = \gamma_{\text{cr}}$, the orbit homoclinic to the hyperbolic fixed point for $x < 0$ is tangential at $d_1(\gamma) = d_3(\gamma)$ to the non-homoclinic stable manifold of the hyperbolic fixed point for $x > 0$. As soon as $\gamma > \gamma_{\text{cr}}$, there is no more intersection of the homoclinic orbit for $x < 0$ with a stable manifold of the hyperbolic fixed point for $x > 0$. This implies that no static π -fluxons can exist. For more details, see [32].

After recalling the description of the π -kinks from [32], we can start the stability analysis. It will be shown that the type 1 π -kink is nonlinearly stable for all $0 \leq \gamma \leq \gamma_{\text{cr}}$. The type 2 and type 3 π -kinks are linearly unstable for all values of γ for which they exist. First we consider the linearization about the π -kinks.

THEOREM 3.1. *The linearizations about the various π -kinks have the following properties:*

(i) *The eigenvalues of the linearization about the monotonic type 1 π -kink $\phi_\pi^1(x; \gamma)$ are strictly negative for $0 \leq \gamma < \gamma_{\text{cr}}$. At $\gamma = \gamma_{\text{cr}}$, the largest eigenvalue is zero. These π -kinks are linearly stable.*

(ii) *The largest eigenvalue of the linearization about the type 2 π -kink $\phi_\pi^2(x; \gamma)$ is strictly positive for $0 < \gamma < \gamma^*$. These π -kinks are linearly unstable.*

(iii) *The largest eigenvalue of the linearization about the type 3 π -kink $\phi_\pi^3(x; \gamma)$ is strictly positive for $0 < \gamma < \gamma_{\text{cr}}$. These π -kinks are linearly unstable. In the limit for $\gamma \rightarrow 0$ and $\gamma \rightarrow \gamma_{\text{cr}}$, the largest eigenvalue converges to zero.*

REMARK 3.2. Note that the instability of the two non-monotonic π -kinks cannot be established by the classical Sturm-Liouville argument. In the classical, autonomous setting, the derivative of the wave about which the system is linearized, is an eigenfunction of the linearized system. This eigenfunction is associated with the translation invariance of the original system and hence corresponds to an eigenvalue $\lambda = 0$. If the wave is non-monotonic, then its derivative has a zero, which implies that $\lambda = 0$ is not the largest eigenvalue [33] and that the wave must be unstable. Due to the discontinuity at $x = 0$, our system is non-autonomous, thus not invariant with respect to translations, and $\lambda = 0$ is (in general) not an eigenvalue. Thus, it cannot a priori be concluded that the non-monotonic π -kinks must be unstable.

To prove Theorem 3.1, it will be shown that the linearization about a π -kink has an eigenvalue zero if and only if the π -kink takes a value which is a multiple of π at $x = 0$. Since the value at $x = 0$ is related to the point $d_i(\gamma)$, it can be derived that this happens only at $\gamma = \gamma_{cr}$ for the colliding type 1 and type 3 waves. To complete the proof, we will derive expressions for the largest eigenvalue of the linearization about each semikink near $\gamma = 0$ in three separate lemmas and use that the eigenvalues are continuous in γ to derive the sign of the largest eigenvalue on the existence interval of the π -kink.

To linearize about a solution $\phi_\pi^i(x; \gamma)$, write $\phi(x, t) = \phi_\pi^i(x; \gamma) + v(x, t)$, substitute this in the model equation (3.1) and disregard all higher order terms:

$$(3.6) \quad [D_{xx} - \cos(\phi_\pi^i(x; \gamma) + \theta(x))]v = D_{tt}v.$$

Using the spectral Ansatz $v(x, t) = e^{\lambda t} \tilde{v}(x)$, where $v(x)$ is a continuously differentiable function and dropping the tildes, we get the eigenvalue problem

$$(3.7) \quad \mathcal{L}^i(x; \gamma)v = \lambda^2 v,$$

where \mathcal{L}^i is defined as

$$(3.8) \quad \mathcal{L}^i(x; \gamma) = D_{xx} - \cos(\phi_\pi^i(x; \gamma) + \theta(x)).$$

The natural domain for \mathcal{L}^i is $H_2(\mathbb{R})$. We call Λ an eigenvalue of \mathcal{L}^i if there is a function $v \in H_2(\mathbb{R})$, which satisfies $\mathcal{L}^i(x; \gamma)v = \Lambda v$. Since \mathcal{L}^i depends smoothly on γ , the eigenvalues of \mathcal{L}^i will depend smoothly on γ too.

The operator \mathcal{L}^i is symmetric, hence all eigenvalues will be real. A straightforward calculation gives that the continuous spectrum of \mathcal{L}^i is in $(-\infty, -\sqrt{1-\gamma^2})$. Since the eigenfunctions are continuously differentiable functions in $H_2(\mathbb{R})$ by the Sobolev Embedding Theorem, Sturm's Theorem [33] can be applied, leading to the fact that the eigenvalues are bounded from above. Furthermore, if v_1 is an eigenfunction of \mathcal{L}^i with eigenvalue Λ_1 and v_2 is an eigenfunction of \mathcal{L}^i with eigenvalue Λ_2 with $\Lambda_1 > \Lambda_2$, then there is at least one zero of v_2 between any pair of zeros of v_1 (including the zeros at $\pm\infty$). Hence if the eigenfunction v_1 has fixed sign, then Λ_1 is the largest eigenvalue of \mathcal{L}^i .

The following lemma gives a necessary and sufficient condition for \mathcal{L}^i to have an eigenvalue $\Lambda = 0$.

LEMMA 3.3. *The eigenvalue problem*

$$\mathcal{L}^i(x; \gamma)v = \Lambda v, \quad x \in \mathbb{R},$$

has an eigenvalue $\Lambda = 0$ if and only if one of the following two conditions holds

- (i) $D_{xx}\phi_\pi^i(x; \gamma)$ is continuous at $x = 0$, i.e., $\phi_\pi^i(0; \gamma) = k\pi$, for some $k \in \mathbb{Z}$;
(ii) $D_x\phi_\pi^i(0; \gamma) = 0$ and there are some x_\pm , with $\text{sgn}(x_\pm) = \pm 1$, such that $D_x\phi_\pi^i(x_\pm; \gamma) \neq 0$.

Proof. Since $\phi_\pi^i(x; \gamma)$ converges to a saddle point for $|x| \rightarrow \infty$, this implies that $D_x\phi_\pi(x; \gamma)$ decays exponentially fast to 0 for $|x| \rightarrow \infty$. Since $\phi_\pi^i(x; \gamma)$ solves (3.3), differentiating this ODE with respect to x , gives

$$\mathcal{L}^i(x; \gamma) D_x\phi_\pi^i(x; \gamma) = 0, \quad \text{for } x \neq 0.$$

This implies that for any constant K , the function $w_K^i(x) = K D_x\phi_\pi^i(x; \gamma)$ satisfies $\mathcal{L}^i(x; \gamma) w_K^i(x) = 0$ for $x \neq 0$. Hence for any K_- and K_+ , the solution

$$w^i(x) = \begin{cases} w_{K_-}^i(x), & x < 0, \\ w_{K_+}^i(x), & x > 0, \end{cases}$$

solves $\mathcal{L}^i(x; \gamma) w^i(x) = 0$ for $x \neq 0$. The function $w^i(x)$ is continuously differentiable if and only if the following two conditions hold

1. $w_{K_-}^i(0-) = w_{K_+}^i(0+)$, in other words, $K_- D_x\phi_\pi^i(0; \gamma) = K_+ D_x\phi_\pi^i(0; \gamma)$, since ϕ_π^i is continuously differentiable;
2. $D_x w_{K_-}^i(0-) = D_x w_{K_+}^i(0+)$, thus $K_- D_{xx}\phi_\pi^i(0-; \gamma) = K_+ D_{xx}\phi_\pi^i(0+; \gamma)$.

The first condition is satisfied if $K_- = K_+$ or $D_x\phi_\pi^i(0; \gamma) = 0$. If $D_x\phi_\pi^i(0; \gamma) = 0$, we can choose K_\pm such that the second condition is satisfied and we do not end up with the trivial solution, except when $D_x\phi_\pi^i(x; \gamma)$ is trivial for either $x > 0$ or $x < 0$.

If $D_x\phi_\pi^i(0; \gamma) \neq 0$, we need $D_{xx}\phi_\pi^i$ to be continuous at $x = 0$ in order to satisfy the second condition. Since $D_{xx}\phi_\pi^i(x; \gamma) = \sin(\phi_\pi^i(x; \gamma) + \theta(x)) - \gamma$, $D_{xx}\phi_\pi^i$ is continuous at $x = 0$ if and only if $\sin(\phi_\pi^i(0; \gamma)) = 0$. These arguments prove that if one of the two conditions are satisfied, then $\Lambda = 0$ is an eigenvalue of \mathcal{L}^i .

Next we assume that $\Lambda = 0$ is an eigenvalue of \mathcal{L}^i , hence there is some continuously differentiable function $v^i(x)$ such that $\mathcal{L}^i(x)v^i(x) = 0$ for $x \neq 0$ and $v^i(x) \rightarrow 0$ for $|x| \rightarrow \infty$. The only solutions decaying to zero at $+\infty$ are the solutions on the one-dimensional stable manifold and similarly, the only solutions decaying to zero at $-\infty$ are the solutions on the one-dimensional unstable manifold. The stable and unstable manifold are formed by multiples of $D_x\phi_\pi^i$. So we can conclude that there exist K_\pm such that

$$v^i(x) = \begin{cases} K_- D_x\phi_\pi^i(x) & \text{for } x < 0, \\ K_+ D_x\phi_\pi^i(x) & \text{for } x > 0. \end{cases}$$

Now we are back in the same situation as above, so we can conclude that either one of the two conditions in the lemma must be satisfied. \square

The second condition in the lemma does not occur. Indeed, the first part of the second condition, i.e., $D_x\phi_\pi^i(0; \gamma) = 0$ happens only if d_i has its second coordinate zero, hence only at $\gamma = \gamma^*$ with $d_2 = d_3$. At this point, the solution $\phi_\pi^2(x; \gamma^*)$ has ceased to exist and the solution $\phi_\pi^3(x; \gamma^*)$ consists of the fixed point for $x > 0$. Hence this solution does not satisfy the second part of the second condition.

To see for which value of γ the first condition is satisfied, we derive the relation between $\phi_\pi^i(0; \gamma)$ and γ . Multiplying the static equation (3.3) with $D_x\phi_\pi^i$ and rewriting it gives

$$D_x[(D_x\phi_\pi^i(x; \gamma))^2] = 2D_x[-\gamma\phi_\pi^i(x; \gamma) - \cos(\phi_\pi^i(x; \gamma) + \theta(x))], \quad x \neq 0.$$

Integration from $\pm\infty$ to 0 and using that $D_x\phi_\pi^i(\pm\infty; \gamma) = 0$, shows

$$\begin{aligned} (D_x\phi_\pi^i(0; \gamma))^2 &= 2[-\gamma(\phi_\pi^i(0; \gamma) - \phi_\pi^i(-\infty; \gamma)) - \cos(\phi_\pi^i(0; \gamma)) + \cos(\phi_\pi^i(-\infty; \gamma))], \\ (D_x\phi_\pi^i(0; \gamma))^2 &= 2[-\gamma(\phi_\pi^i(0; \gamma) - \phi_\pi^i(+\infty; \gamma)) + \cos(\phi_\pi^i(0; \gamma)) - \cos(\phi_\pi^i(+\infty; \gamma))]. \end{aligned}$$

Subtracting these two equations and using that $\phi_\pi^i(+\infty; \gamma) = \phi_\pi^i(-\infty; \gamma) + \pi$, we get that

$$(3.9) \quad 0 = -\pi\gamma - 2\cos(\phi_\pi^i(0; \gamma)), \quad \text{hence} \quad \cos(\phi_\pi^i(0; \gamma)) = \frac{\pi\gamma}{2}.$$

Thus the first condition is only satisfied when $\cos(\phi_\pi^i(0; \gamma)) = \pm 1$, hence $\gamma = \frac{2}{\pi} = \gamma_{\text{cr}}$.

The following step in the analysis of the eigenvalues of the linearization is to consider the behavior of the eigenvalues for γ small. First note that at $\gamma = 0$, we have an explicit expression for the π -fluxon and the 3π -fluxon (see (3.2) for the expression of ϕ_{flux}):

$$(3.10) \quad \phi_\pi^1(x; 0) = \begin{cases} \phi_{\text{flux}}(x - \ln(1 + \sqrt{2})), & \text{for } x < 0, \\ \pi - \phi_{\text{flux}}(-x - \ln(1 + \sqrt{2})), & \text{for } x > 0, \end{cases}$$

$$(3.11) \quad \phi_{3\pi}^2(x; 0) = \begin{cases} \phi_{\text{flux}}(x + \ln(1 + \sqrt{2})), & \text{for } x < 0, \\ 3\pi - \phi_{\text{flux}}(-x + \ln(1 + \sqrt{2})), & \text{for } x > 0. \end{cases}$$

Hence the derivatives of both functions are even and $\cos(\phi_\pi^i(x; 0) + \theta)$ is continuous and even, since $\phi_\pi^1(0; 0) = \frac{\pi}{2}$ and $\phi_{3\pi}^2(0; 0) = \frac{3\pi}{2}$.

For $\gamma \ll 1$, the homoclinic orbit in the system with $\theta = 0$ will be crucial for the approximation of type 2 and type 3 solutions. This orbit is homoclinic to $\arcsin(\gamma)$ and will be denoted by $\phi_h(x; \gamma)$. It can be approximated up to order γ by using the 2π -fluxon ϕ_{flux} and its linearization.

LEMMA 3.4. *For γ small, we have for the even homoclinic connection $\phi_h(x; \gamma)$*

$$(3.12) \quad \phi_h(x; \gamma) = \phi_{\text{flux}}(x + L_\pi(\gamma)) + \gamma\phi_1(x + L_\pi(\gamma)) + \gamma^2 R_2(x + L_\pi(\gamma); \gamma), \quad x < 0,$$

where the expression for the 2π -fluxon ϕ_{flux} can be found in (3.2),

$$\phi_1(x) = \frac{1}{2} \left[-1 + \cosh x + \int_0^x \frac{\xi}{\cosh \xi} d\xi \right] \frac{1}{\cosh x} - \arctan e^x \left(\frac{x}{\cosh x} + \sinh x \right)$$

and $L_\pi(\gamma)$ is such that $\phi_h(-L_\pi(\gamma); \gamma) = \pi = \phi_{\text{flux}}(0)$, implying

$$(3.13) \quad L_\pi(\gamma) = \frac{1}{2} |\ln \gamma| + \ln \frac{4}{\sqrt{\pi}} + \mathcal{O}(\sqrt{\gamma}).$$

Furthermore, $\gamma^2 R_2(x + L_\pi(\gamma); \gamma) = \mathcal{O}(\gamma)$, uniform for $x < 0$ and $\gamma\phi_1(L_\pi(\gamma); \gamma) = \mathcal{O}(\sqrt{\gamma})$. Thus

$$(3.14) \quad \phi_h(0) = 2\pi - 2\sqrt{\pi}\sqrt{\gamma} + \mathcal{O}(\gamma).$$

Finally, $\phi_1(\tilde{x}; \gamma) = \mathcal{O}(1)$ and $R_2(\tilde{x}; \gamma) = \mathcal{O}(1)$, uniform for $\tilde{x} < 0$.

Proof. It is more convenient in the following perturbation analysis to follow the normalization of $\phi_{\text{flux}}(x)$, i.e., in this proof we introduce new coordinates $\tilde{x} = x + L_\pi(\gamma)$ where $L_\pi(\gamma)$ is such that $\phi_h(-L_\pi(\gamma); \gamma) = \pi = \phi_{\text{flux}}(0)$. In the following we will drop the tildes and work in those new coordinates. As ϕ_h in the original coordinates was

even, we get in the new coordinates $D_x \phi_h(L_\pi(\gamma); \gamma) = 0$. This condition will be used later to determine an asymptotic expression for $L_\pi(\gamma)$.

In the new coordinates, we introduce the expansion

$$\phi_h(x; \gamma) = \phi_{\text{flux}}(x) + \gamma \phi_1(x) + \gamma^2 R_2(x; \gamma), \quad x < L_\pi(\gamma).$$

By linearizing about ϕ_{flux} , it follows that the equation for ϕ_1 is

$$(3.15) \quad \mathcal{L}(x) \phi_1 = -1, \quad \text{where} \quad \mathcal{L}(x) = D_{xx} - \cos(\phi_{\text{flux}}(x)).$$

The operator $\mathcal{L}(x)$ is identical to the operator associated with the stability of $\phi_{\text{flux}}(x)$. The homogeneous problem $\mathcal{L}\psi = 0$ has the following two independent solutions,

$$(3.16) \quad \psi_b(x) = \frac{1}{\cosh x}, \quad \psi_u(x) = \frac{x}{\cosh x} + \sinh x,$$

where $\psi_b(x) = \frac{1}{2} \frac{d}{dx} \phi_{\text{flux}}(x)$ is bounded and $\psi_u(x)$ unbounded as $x \rightarrow \pm\infty$. By the variation-of-constants method, we find the general solution to (3.15),

$$\begin{aligned} \phi_1(x; A, B) = & \left[A + \frac{1}{2} \cosh x + \frac{1}{2} \int_0^x \frac{\xi}{\cosh \xi} d\xi \right] \frac{1}{\cosh x} \\ & + [B - \arctan e^x] \left(\frac{x}{\cosh x} + \sinh x \right), \end{aligned}$$

with $A, B \in \mathbb{R}$. The solution $\phi_1(x)$ of (3.15) must be bounded as $x \rightarrow -\infty$ and is normalized by $\phi_1(0) = 0$ (since $\phi_h(0) = \phi_{\text{flux}}(0) = \pi$). Thus, we find that $A = -\frac{1}{2}$ and $B = 0$. Note that $\lim_{x \rightarrow -\infty} \phi_1(x) = 1$, which agrees with the fact that $\lim_{x \rightarrow -\infty} \phi_h(x) = \arcsin \gamma = \gamma + \mathcal{O}(\gamma^3)$. The solution $\phi_1(x)$ is clearly not bounded as $x \rightarrow \infty$, the unbounded parts of $\phi_1(x)$ and $\frac{d}{dx} \phi_1(x)$ are given by

$$(3.17) \quad \phi_1|_u(x) = -\arctan e^x \sinh x, \quad \frac{d}{dx} \phi_1|_u(x) = -\arctan e^x \cosh x.$$

It follows that $\phi_1(x) = \mathcal{O}(\gamma^{-\sigma})$ for some $\sigma > 0$ if $e^x = \mathcal{O}(\gamma^{-\sigma})$, i.e., if $x = \sigma |\ln \gamma|$ at leading order. Using this, it is a straightforward procedure to show that the rest term $\gamma^2 R_2(x; \gamma)$ in (3.12) is of $\mathcal{O}(\gamma^{2-2\sigma})$ for $x = \sigma |\ln \gamma| + \mathcal{O}(1)$ (and $\sigma > 0$). Hence, the approximation of $\phi_h(x)$ by expansion (3.12) breaks down as x becomes of the order $|\ln \gamma|$. On the other hand, it also follows that $\phi_{\text{appr}}^1(x) = \phi_{\text{flux}}(x) + \gamma \phi_1(x)$ is a uniform $\mathcal{O}(\gamma)$ -accurate approximation of $\phi_h(x)$ on an interval $(-\infty, L]$ for $L = \frac{1}{2} |\ln \gamma| + \mathcal{O}(1)$. Since $\phi_{\text{flux}}(L) + \gamma \phi_1(L) = \mathcal{O}(\sqrt{\gamma})$ for such L , we can compute $L_\pi = \frac{1}{2} |\ln \gamma| + \mathcal{O}(1)$, as L_π is the value of x at which

$$0 = \frac{d}{dx} \phi_h(x) = \frac{d}{dx} \phi_{\text{appr}}^1(x) + \mathcal{O}(\gamma) = \frac{d}{dx} \phi_{\text{flux}}(x) + \gamma \frac{d}{dx} \phi_1|_u(x) + \mathcal{O}(\gamma).$$

We introduce Y by $e^x = \frac{Y}{\sqrt{\gamma}}$, so that it follows by (3.2) and (3.17) that $Y = \frac{4}{\sqrt{\pi}} + \mathcal{O}(\sqrt{\gamma})$, i.e.

$$L_\pi(\gamma) = \frac{1}{2} |\ln \gamma| + \ln \frac{4}{\sqrt{\pi}} + \mathcal{O}(\sqrt{\gamma}).$$

A straightforward calculation shows that (in the new coordinates)

$$\phi_h(L_\pi) = 2\pi - 2\sqrt{\pi}\sqrt{\gamma} + \mathcal{O}(\gamma).$$

As $\phi_h(x)$ and $\phi_{\text{flux}}(x)$ both converge exponentially fast to fixed points which are order γ apart for $x \rightarrow -\infty$, it follows immediately that $\phi_1(x; \gamma) = \mathcal{O}(1)$ and $R_2(x; \gamma) = \mathcal{O}(1)$, uniform for $x < 0$. \square

Now we are ready to consider the stability of the various types of π -fluxons individually.

3.1. Stability of the type 1 solution. LEMMA 3.5. *For all $0 \leq \gamma < \gamma_{\text{cr}}$, all eigenvalues of $\mathcal{L}^1(x; \gamma)$ are strictly negative. For $\gamma = \gamma_{\text{cr}}$, the operator $\mathcal{L}^1(x; \gamma_{\text{cr}})$ has 0 as its largest eigenvalue. For $\gamma = 0$, the largest eigenvalue is $-\frac{1}{4}(\sqrt{5} + 1)$. Furthermore, for all $0 \leq \gamma < \gamma_{\text{cr}}$, the type 1 semikinks $\phi_\pi^1(x; \gamma)$ are Lyapunov stable in the following sense. For all $\varepsilon > 0$, there is some $\delta > 0$ such that any solution $\phi(x, t)$ of the semi-fluxon equation (3.1), which is convergent to 0 at $x \rightarrow -\infty$ and to π at $x \rightarrow +\infty$ and which satisfies initially $\|\phi(\cdot, 0) - \phi_\pi^1(\cdot; \gamma)\|_{H^1} + \|\phi_t(\cdot, 0)\|_{L^2} < \delta$ will satisfy $\|\phi(\cdot, t) - \phi_\pi^1(\cdot; \gamma)\|_{L^2} + \|\phi_t(\cdot, t)\|_{L^2} < \varepsilon$ for all $t \in \mathbb{R}$.*

Proof. From Lemma 3.3 it follows that \mathcal{L}^1 has an eigenvalue $\Lambda = 0$ at $\gamma = \gamma_{\text{cr}}$. The eigenfunction is $D_x \phi_\pi^1(x; \gamma_{\text{cr}})$ and this function is always positive, since $\phi_\pi^1(x; \gamma_{\text{cr}})$ is monotonically increasing. From Sturm's Theorem, it follows that $\Lambda = 0$ is the largest eigenvalue of \mathcal{L}^1 at $\gamma = \gamma_{\text{cr}}$. Next we consider $\gamma = 0$. We can explicitly determine all eigenvalues of $\mathcal{L}^1(x; 0)$. From the explicit expression for ϕ_π^1 it follows that $\mathcal{L}^1(x; 0)$ is a continuous even operator. For fixed Λ , the operator $\mathcal{L}^1(x; 0) - \Lambda$ has two linearly independent solutions. Since the fixed point is a saddle point and the decay rate to this fixed point is like e^{-x} , there is one solution that is exponentially decaying at $+\infty$ and there is one solution that is exponentially decaying at $-\infty$, if $\Lambda > -1$. If we denote the exponentially decaying function at $-\infty$ by $v_-(x; \Lambda)$, then the exponentially decaying function at $+\infty$ up to a constant is given by $v_+(x; \Lambda) = v_-(-x; \Lambda)$ (since \mathcal{L}^1 is symmetric in x). Obviously, $v_+(0; \Lambda) = v_-(0; \Lambda)$, hence Λ is an eigenvalue if $D_x v_+(0; \Lambda) = D_x v_-(0; \Lambda)$, (i.e., when $D_x v_-(0; \Lambda) = 0$) or if $v_-(0; \Lambda) = 0$.

Using [22], we can derive explicit expression for the solutions $v_-(x; \Lambda)$ (see also [10]). Using $x_1 = \ln(\sqrt{2} + 1)$, we have

$$v_-(x; 0) = \text{sech}(x - x_1), \quad v_-(x; \Lambda) = e^{\mu(x - x_1)} [\tanh(x - x_1) - \mu], \quad \mu = \sqrt{\Lambda + 1}.$$

A straightforward calculation shows that $v_-(0; \Lambda) \neq 0$. The condition $D_x v_-(0; \Lambda) = 0$ gives that

$$\mu^2 - \frac{1}{2}\sqrt{2}\mu - \frac{1}{2} = 0, \quad \text{hence} \quad \sqrt{\Lambda + 1} = \frac{1}{4}\sqrt{2}(\sqrt{5} - 1) \Rightarrow \Lambda = -\frac{1}{4}(\sqrt{5} + 1).$$

Now assume that the operator $\mathcal{L}^1(x; \gamma)$ has a positive eigenvalue $\Lambda^1(\gamma)$ for some $0 \leq \gamma < \gamma_{\text{cr}}$. Since Λ depends continuously on γ , there has to be some $0 < \hat{\gamma} < \gamma_{\text{cr}}$ such that $\Lambda^1(\hat{\gamma}) = 0$. However, from Lemma 3.3 it follows that this is not possible.

Nonlinear or Lyapunov stability can be derived by looking at the ‘‘temporal Hamiltonian’’

$$\mathcal{H}(\phi, p) = \int_{-\infty}^{\infty} \left[\frac{1}{2}p^2 + \frac{1}{2}(\phi_x)^2 - \cos(\phi + \theta) - \gamma(\phi + \theta) \right] dx$$

This functional is a Lyapunov function for the system (3.1), i.e., any solution $\phi(x, t) \in H^2(\mathbb{R})$ of (3.1) satisfies $\frac{d}{dt}\mathcal{H}(\phi, \phi_t) = 0$, hence $\mathcal{H}(\phi(\cdot, t), \phi_t(\cdot, t)) = \mathcal{H}(\phi(\cdot, 0), \phi_t(\cdot, 0))$ for any $t \in \mathbb{R}$. Furthermore, the linearization $D^2\mathcal{H}$ at $(\phi, p) = (\phi_\pi^1, 0)$ (the point related to the π -fluxon) is given by

$$D^2\mathcal{H}(\phi_\pi^1, 0) = \begin{pmatrix} -\mathcal{L}^1(x; \gamma) & 0 \\ 0 & I \end{pmatrix},$$

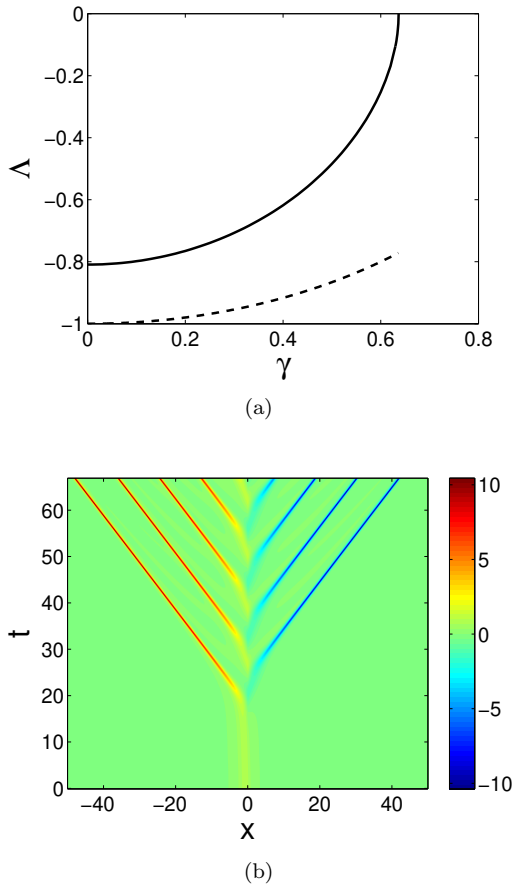


FIG. 3.2. (a) The eigenvalue of linear operator associated to the type 1 semifluxon as a function of the bias current γ . The dashed line is the boundary of the continuous spectrum. (b) A simulation of the evolution of a π -kink in the presence of a bias current above the critical value ($\gamma > \gamma_{\text{cr}}$). The plot presents the magnetic field ϕ_x . The numerics show that the instability leads to the release of wave trains of traveling wave fluxons. In this evolution a damping, which is proportional to ϕ_t , has been applied to the system.

which is a strictly positive definite self-adjoint operator on $L_2(\mathbb{R}) \times L_2(\mathbb{R})$ with domain $H_2(\mathbb{R}) \times L_2(\mathbb{R})$. So there is some $c > 0$ such that for any $(\phi, p) \in H_2 \times L_2$, we have $H(\phi, p) - H(\phi_\pi^1, 0) \geq c(\|\phi - \phi_\pi^1\|_{L_2}^2 + \|p\|_{L_2}^2)$, see e.g. [15, 36]. Finally, it is straightforward to prove that there is some $C > 0$ such that $H(\phi, p) - H(\phi_\pi^1, 0) \leq C(\|\phi - \phi_\pi^1\|_{H_1}^2 + \|p\|_{L_2}^2)$ for any $(\phi, p) \in H_2 \times L_2$. \square

Using standard procedures in MATLAB, the eigenvalues of the type 1 π -fluxon have been calculated numerically as a function of the applied bias current γ and are presented in Figure 3.2(a). Further details of the computational procedure are presented in section 6. Figure 3.2(a) shows that the type 1 semifluxon has only one eigenvalue. This eigenvalue tends to zero when the bias current γ approaches the critical value γ_{cr} as has been derived analytically. It was first proposed in [16, 20] that a constant driving force can excite the largest eigenvalue of a semifluxon toward zero.

When we apply a bias current above the critical value γ_{cr} , numerics show that the

stationary π -kink bifurcates into a semifluxon that reverses its polarity and releases a fluxon. This process keeps repeating itself: the semifluxon changes its direction back and forth with releasing a fluxon or antifluxon in every change. A simulation of the release of fluxons from a semifluxon is presented in Figure 3.2(b). In experiments, the polarity of a semifluxon can also be reversed by applying a magnetic field [14].

When $\gamma = \gamma_{\text{cr}}$, the type 1 and type 3 semifluxons coincide. From the numerical analysis of the eigenvalues of the type 3 semifluxon (see section 3.3 for details), it follows that there is an eigenvalue at the edge of the continuous spectrum for $\gamma = \gamma_{\text{cr}}$. We conjecture that this eigenvalue bifurcates into the edge of the continuous spectrum at this point as γ increases to γ_{cr} (see Figure 3.4).

3.2. Instability of type 2 solutions. LEMMA 3.6. *For all $0 < \gamma < \gamma^*$, the largest eigenvalue of $\mathcal{L}^2(x; \gamma)$ is strictly positive. In the limit $\gamma \rightarrow 0$, the largest eigenvalue of $\mathcal{L}^2(x; \gamma)$ converges to $\frac{1}{4}(\sqrt{5} - 1)$.*

Proof. Using the approximation for the homoclinic orbit $\phi_h(x; \gamma)$ in Lemma 3.4, we see that, for γ small, an approximation for the π -fluxon of type 2 is given by (as before, $x_1 = \ln(1 + \sqrt{2})$)

$$(3.18) \quad \phi_\pi^2(x; \gamma) = \begin{cases} \phi_{\text{flux}}(x + x_1) + \mathcal{O}(\gamma), & x < 0 \\ \pi + \phi_{\text{flux}}(\tilde{x}) + \gamma\phi_1(\tilde{x}) + \gamma^2 R_2(\tilde{x}; \gamma), & 0 < x < L_\pi(\gamma) + x_1 \\ \pi + \phi_{\text{flux}}(-\hat{x}) + \gamma\phi_1(-\hat{x}) + \gamma^2 R_2(-\hat{x}; \gamma), & x > L_\pi(\gamma) + x_1 \end{cases}$$

with $\tilde{x} = x - x_1$ and $\hat{x} = x - 2L_\pi(\gamma) - x_1$.

There is no limit for $\gamma \rightarrow 0$, since the semifluxon breaks in two parts, one of them being the 3π -fluxon $\phi_{3\pi}^2(x; 0)$. In a similar way as we found the largest eigenvalue for the linearization operator $\mathcal{L}^1(x; 0)$ about the π -fluxon $\phi_\pi^1(x; 0)$, we can find the largest eigenvalue for the linearization operator $\mathcal{L}^2(x; 0)$ about the 3π -fluxon $\phi_{3\pi}^2(x; 0)$. The largest eigenvalue is $\Lambda^2(0) = \frac{1}{4}(\sqrt{5} - 1)$ and the eigenfunction is

$$\psi^2(x; 0) = \begin{cases} e^{\mu_0(x+x_1)}(\mu_0 - \tanh(x + x_1)), & x < 0, \\ e^{\mu_0(-x+x_1)}(\mu_0 - \tanh(-x + x_1)), & x > 0, \end{cases}$$

where $\mu_0 = \sqrt{\Lambda^2(0) + 1} = \frac{1}{4}\sqrt{2}(1 + \sqrt{5})$. (It can be shown that there is another smaller eigenvalue $\Lambda = -\frac{1}{2}$ and similar eigenfunction if $\mu = \frac{1}{2}\sqrt{2} = \tanh(x_1)$, see Remark 3.8.)

In a similar way, using the approximation (3.18) for $\phi_\pi^2(x; \gamma)$, the eigenfunction of an eigenvalue of ϕ_π^2 for γ small is approximated by

$$\psi^2(x; \gamma) = \begin{cases} e^{\mu(x+x_1)}(\mu - \tanh(x + x_1)) + \mathcal{O}(\sqrt{\gamma}), & x < 0 \\ k_2 e^{-\mu\tilde{x}}(\mu - \tanh(-\tilde{x})) + k_3 e^{\mu\tilde{x}}(\mu - \tanh\tilde{x}) + \mathcal{O}(\sqrt{\gamma}), & 0 < x < L_\pi(\gamma) + x_1 \\ k_4 e^{\mu(-\hat{x})}(\mu + \tanh\hat{x}) + \mathcal{O}(\sqrt{\gamma}), & x > L_\pi(\gamma) + x_1. \end{cases},$$

where k_i and μ have to be determined. The eigenvalue Λ follows from $\mu = \sqrt{\Lambda^2 + 1}$. Note that the secular term which is growing at infinity with the multiplication factor k_3 is included in this approximation. When $\gamma = 0$ and $k_3 = 0$, the first two lines in the definition of ψ^2 are the eigenfunction of the linearized problem about the heteroclinic connection between 0 and 3π , as presented above. When γ is nonzero, k_3 can be of order $\mathcal{O}(\gamma^\sigma)$ for $\sigma > \frac{\mu}{2}$ as the secular term is of order $\mathcal{O}(\gamma^{-\mu/2})$ at $x = L_\pi(\gamma) + x_1$.

The constants k_2 , k_3 and k_4 and the parameter μ have to be chosen such that for $\gamma > 0$ (but small) the function $\psi^2(x, \gamma)$ is continuously differentiable at $x = 0$ and

$x = L_\pi(\gamma) + x_1$. From the continuity conditions at $x = 0$, we obtain:

$$k_2 = \frac{\sqrt{2}}{4\mu(\mu-1)(\mu+1)} + \mathcal{O}(\sqrt{\gamma}),$$

$$k_3 = \frac{(3+2\sqrt{2})^\mu(2\mu^2-\mu\sqrt{2}-1)(2\mu-\sqrt{2})}{4\mu(\mu^2-1)} + \mathcal{O}(\sqrt{\gamma}).$$

From one of the continuity conditions at $x = L_\pi(\gamma) + x_1$, we obtain $k_4 = k_4(k_2, k_3, \mu)$. Now we are left with one more matching condition. Values of μ for which this condition is satisfied correspond to the eigenvalues of the operator $\mathcal{L}^2(x; \gamma)$ for γ small. More explicitly, the spectral parameter μ has to satisfy the equation

$$(3.19) \quad \mathcal{F}(\mu) = 16^\mu k_3 (\mu-1)^2 (\gamma\pi)^{-\mu} ((3\mu+4)\pi\gamma + 16\mu) + \mathcal{O}(\gamma^{-\mu+2}) = 0.$$

Note that this expression is not defined at $\gamma = 0$. This corresponds to the singularities in the expression for ϕ^2 as $\gamma \rightarrow 0$ due to the fact that $L_\pi(\gamma) \rightarrow \infty$ for $\gamma \rightarrow 0$. Evaluating $\mathcal{F}(\mu) (\gamma\pi)^\mu$ at $\gamma = 0$, we see that there are four positive roots for μ , leading to four squared eigenvalues, namely $\Lambda(0) = \frac{1}{4}(\sqrt{5}-1)$, $-\frac{1}{2}$, and the double eigenvalue $\Lambda(0) = 0$. The first two come from the zeros of k_3 and are related to the eigenvalues of the 3π -fluxon. The double zero eigenvalues are the eigenvalues of the fluxon. One can also notice that there is no term with a multiplication factor k_2 to this leading order. This term appears at most of order $\mathcal{O}(\gamma^{\mu+2})$. Finally, as with the type 1 semi-fluxon, the root $\mu = 0$ corresponds to the edge of the continuous spectrum and the ‘‘eigenfunction’’ is not in $H_2(\mathbb{R})$.

The proof that the largest eigenvalue is near $\frac{1}{4}(\sqrt{5}-1)$ for γ small will be complete if we can show that $\mathcal{F}_\mu(\frac{\sqrt{2}}{4}(1+\sqrt{5})) \neq 0$, i.e. the non-degeneracy condition that says that the eigenvalue can be continued continuously for γ small.

Simple algebraic calculations give that

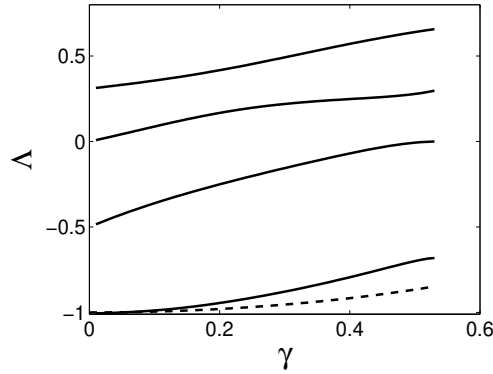
$$(3.20) \quad \mathcal{F}_\mu\left(\frac{\sqrt{2}}{4}(1+\sqrt{5})\right) = c_1 \gamma^{-\frac{\sqrt{2}}{4}(1+\sqrt{5})} + \mathcal{O}(\gamma^{1-\frac{\sqrt{2}}{4}(1+\sqrt{5})})$$

with c_1 a positive constant. Hence, $\mathcal{F}_\mu(\frac{\sqrt{2}}{4}(1+\sqrt{5})) > 0$.

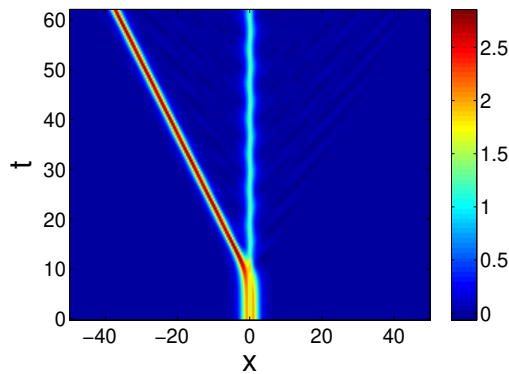
This completes the proof that the largest eigenvalue is near $\frac{1}{4}(\sqrt{5}-1)$ for small but positive γ . Since the largest eigenvalue depends continuously on γ , it can only disappear at a bifurcation point. There are no bifurcation points and it is not possible that the eigenvalue becomes 0 (see Lemma 3.3), hence the largest eigenvalue will be positive as long as fluxon $\phi_\pi^2(x; \gamma)$ exists, i.e., for $0 < \gamma < \gamma^*$. \square

REMARK 3.7. We cannot use a comparison theorem, because $\phi_\pi^2 < \phi_\pi^3$ for $x < 0$ and $\phi_\pi^2 > \phi_\pi^3$ for $x > 0$.

To consider the relation between the eigenvalues of $\mathcal{L}^2(x; \gamma)$ and the stability problem of $\phi_\pi^2(x; \gamma)$, we denote the largest eigenvalue of $\mathcal{L}^2(x; \gamma)$ by $\Lambda^2(\gamma)$. The associated eigenvalues for the linearizations are solution of the equation $\lambda^2 - \Lambda^2(\gamma) = 0$, hence $\lambda = \pm\sqrt{\Lambda^2(\gamma)}$. Since $\Lambda^2(\gamma) > 0$, this implies that one of the two eigenvalues has positive real part, hence the π -fluxons of type 2 are unstable. The numerically obtained eigenvalues of semifluxons of this type as a function of γ are shown in Figure 3.3(a). In the proof of Lemma 3.6 we have found three different eigenvalues for γ small and the possibility of a fourth eigenvalue coming out of the continuous spectrum at $\gamma = 0$. In Figure 3.3(a), we see the continuation of those eigenvalues. In Figure 3.3(b), we present the evolution of a 3π -kink (3.11) which is the limit of a type



(a)



(b)

FIG. 3.3. (a) The eigenvalues of the linear operator associated to the type 2 semifluxon as a function of the bias current γ . The result that the largest eigenvalue is always positive shows the instability of type 2 semifluxon. When $\gamma \rightarrow 0$, $\Lambda \rightarrow \frac{1}{4}(\sqrt{5} - 1)$ which is the largest eigenvalue of a 3π -kink. At $\gamma = 0$, one eigenvalue comes out of the edge of the continuous spectrum (dashed line). (b) The evolution of a 3π -kink (3.11) for $\gamma = 0$. The plot is presented in terms of the magnetic field ϕ_x . The separation of a fluxon from the semifluxon can be clearly seen.

2 semifluxon when $\gamma \rightarrow 0$. The separation of a fluxon from the semifluxon is clearly seen and indicates the instability of the state (which confirms the analysis in the proof of Lemma 3.6).

REMARK 3.8. A type 2 semifluxon can be seen as a concatenation of a 3π - and a -2π -kink in the limit $\gamma \rightarrow 0$. In that limit the other eigenvalues of $\mathcal{L}^2(x; \gamma)$ converge to 0, $-\frac{1}{2}$, and -1 . The eigenvalues 0 and -1 are contributions of the -2π -kink. The eigenvalue $-\frac{1}{2}$ corresponds to the first excited state of the 3π -kink with eigenfunction

$$\psi^2(x; 0) = \begin{cases} e^{\mu(x+x_1)}(\mu - \tanh(x+x_1)), & x < 0, \\ e^{\mu(-x+x_1)}(\tanh(-x+x_1) - \mu), & x > 0, \end{cases}$$

where $\mu = \sqrt{\Lambda + 1} = \frac{1}{\sqrt{2}}$.

3.3. Instability of type 3 solutions. LEMMA 3.9. For all $0 < \gamma < \gamma_{\text{cr}}$, the largest eigenvalue of $\mathcal{L}^3(x; \gamma)$ is strictly positive. For $\gamma = \gamma_{\text{cr}}$, the operator $\mathcal{L}^3(x; \gamma_{\text{cr}})$

has 0 as its largest eigenvalue.

Proof. The solution $\phi_\pi^3(x, \gamma_{\text{cr}}) = \phi_\pi^1(x, \gamma_{\text{cr}})$, hence from Lemma 3.5 it follows that the largest eigenvalue is $\Lambda = 0$.

For γ near zero, we will use the approximation for the homoclinic orbit $\phi_h(x; \gamma)$ in Lemma 3.4 to get an approximation for the type 3 fluxon

$$\phi_\pi^3(x; \gamma) = \begin{cases} \phi_{\text{appr}}^1(\hat{x}) = \phi_{\text{flux}}(\hat{x}) + \gamma\phi_1(\hat{x}) + \gamma^2 R_2(\hat{x}; \gamma), & x < -L_\pi(\gamma) + x_1, \\ \phi_{\text{appr}}^2(\tilde{x}) = \phi_{\text{flux}}(-\tilde{x}) + \gamma\phi_1(-\tilde{x}) + \gamma^2 R_2(-\tilde{x}; \gamma), & -L_\pi(\gamma) + x_1 < x < 0, \\ \phi_{\text{appr}}^3(-x - x_1) = \pi + \phi_{\text{flux}}(-x - x_1) + \mathcal{O}(\gamma), & x > 0, \end{cases}$$

where $\tilde{x} = x - x_1$ and $\hat{x} = x - x_1 + 2L_\pi(\gamma)$.

In the limit $\gamma \rightarrow 0$, the type 3 semi-fluxon break into a type 1 semi-fluxon and a fluxon. Both are stable and the largest eigenvalue of the fluxon is zero, while the largest eigenvalue of the type 1 semi-fluxon is negative. Hence to approximate the largest eigenvalue of the type 3 semi-fluxon for γ small, we set

$$\Lambda(\gamma) = \gamma\Lambda_1(\gamma).$$

To construct the first part of the approximation of the eigenfunction, we consider $x < -L_\pi(\gamma) + x_1$, i.e., $\hat{x} < L_\pi(\gamma)$. In this part of the arguments, we will drop the hat in \hat{x} . On $(-\infty, L_\pi)$, we expand $\psi_{\text{approx}}^1 = \psi_0 + \gamma\psi_1$, this yields the following equations for $\psi_{0,1}(x)$,

$$(3.21) \quad \mathcal{L}\psi_0 = 0, \quad \mathcal{L}\psi_1 = [\Lambda_1(0) - \phi_1(x) \sin \phi_{\text{flux}}(x)]\psi_0.$$

As ψ_{approx}^1 has to be an eigenfunction, we have $\psi_{\text{approx}}^1(x) \rightarrow 0$ as $x \rightarrow -\infty$. Furthermore, we remove the scaling invariance by assuming that $\psi_{\text{approx}}^1(0) = 1$. This implies that $\psi_0(x)$ is given by

$$(3.22) \quad \psi_0(x) = \frac{1}{\cosh x}$$

(see 3.16). To solve the ψ_1 -equation, we note that $\frac{d}{dx}\phi_1(x)$ is a solution of

$$\mathcal{L}\psi = -\phi_1 \sin \phi_{\text{flux}} \frac{d}{dx}\phi_{\text{flux}} = -2\phi_1 \sin \phi_{\text{flux}}\psi_0,$$

(see (3.15) and (3.2)) so that we find as general solution,

$$\begin{aligned} \psi_1(x) = & \left[A - \frac{1}{2}\Lambda_1(\ln(\cosh x) + \int_0^x \frac{\xi}{\cosh^2 \xi} d\xi) \right] \frac{1}{\cosh x} \\ & + \left[B + \frac{1}{2}\Lambda_1 \tanh x \right] \left(\frac{x}{\cosh x} + \sinh x \right) + \frac{1}{2} \frac{d}{dx}\phi_1. \end{aligned}$$

Using $\lim_{x \rightarrow -\infty} \psi_1(x) = 0$ and $\psi_1(0) = 0$ we find that $A = \frac{\pi}{4}$, $B = \frac{1}{2}\Lambda_1(0)$. As in the case of $\phi_1(x)$, we are especially interested in the unbounded parts of $\psi_1(x)$ and $\frac{d}{dx}\psi_1(x)$,

$$(3.23) \quad \begin{aligned} \psi_1|_u(x) &= \frac{1}{2}\Lambda_1(1 + \tanh x) \sinh x - \frac{1}{2} \arctan e^x \cosh x, \\ \frac{d}{dx}\psi_1|_u(x) &= \frac{1}{2}\Lambda_1(1 + \tanh x) \cosh x - \frac{1}{2} \arctan e^x \sinh x. \end{aligned}$$

We note that the error term $|\psi(x) - \psi_{\text{appr}}^1(x)| = \gamma^2 |S_2(x; \gamma)|$ is at most $\mathcal{O}(\gamma)$ on $(-\infty, L_\pi)$ (the analysis is similar to that for $\gamma^2 |R_2(x; \gamma)|$).

Next consider the second part of the approximation, i.e., x between $-L_\pi(\gamma) + x_1$ and 0. Here we define the translated coordinate $\tilde{x} = x - x_1$, which is on the interval $(-L_\pi, -x_1)$ and again we drop the tildes. Since we have to match $\psi_{\text{appr}}^1(x)$ to the approximation $\psi_{\text{appr}}^2(x)$ of $\psi(x)$, along $\phi_{\text{appr}}^2(x)$ and thus defined on the interval $(-L_\pi, -x_1)$, we need to compute $\psi_{\text{appr}}^1(L_\pi)$ and $\frac{d}{dx}\psi_{\text{appr}}^1(L_\pi)$ which to the leading order are calculated from (3.23), i.e.

$$(3.24) \quad \psi_{\text{appr}}^1(L_\pi) = \frac{2\Lambda_1(0)}{\sqrt{\pi}}\sqrt{\gamma} + \mathcal{O}(\gamma), \quad \frac{d}{dx}\psi_{\text{appr}}^1(L_\pi) = \frac{2\Lambda_1(0) - \pi}{\sqrt{\pi}}\sqrt{\gamma} + \mathcal{O}(\gamma).$$

Thus, both $\psi_{\text{appr}}^1(L_\pi)$ and $\frac{d}{dx}\psi_{\text{appr}}^1(L_\pi)$ are $\mathcal{O}(\sqrt{\gamma})$.

Now, we choose a special form for $\psi_{\text{appr}}^2(x)$, the continuation of $\psi(x)$, i.e. the part linearized along $\phi_{\text{appr}}^2(x)$. It is our aim to determine the value of Λ_1 , for which there exists a positive integrable C^1 solution ψ of $\mathcal{L}^3(x; \gamma)\psi = \gamma\Lambda_1(0)\psi$. By general Sturm-Liouville theory [33] we know that this value of Λ_1 must be the largest eigenvalue. Our strategy is to try to continue $\psi(x)$ beyond $(-\infty, L_\pi)$ by a function that remains at most $\mathcal{O}(\sqrt{\gamma})$, i.e. we do not follow the approach of the existence analysis and thus do not reflect and translate $\psi_{\text{appr}}^1(x)$ to construct $\psi_{\text{appr}}^2(x)$ (since this solution becomes in general $\mathcal{O}(1)$ for $x = \mathcal{O}(1)$). Instead, we scale $\psi_{\text{appr}}^2(x)$ as $\gamma\tilde{\psi}(x)$. The linearization $\tilde{\psi}(x)$ along $\phi_{\text{appr}}^2(x)$ on the interval $(-L_\pi, x_1)$ must solve $\mathcal{L}\tilde{\psi} = \mathcal{O}(\gamma)$, thus, at leading order

$$(3.25) \quad \tilde{\psi}(x) = \frac{\tilde{A}}{\cosh x} + \tilde{B} \left(\frac{x}{\cosh x} + \sinh x \right).$$

The approximation $\psi_{\text{appr}}^2(x) = \gamma\tilde{\psi}(x)$ must be matched to $\psi_{\text{appr}}^1(L_\pi)$ and $\frac{d}{dx}\psi_{\text{appr}}^1(L_\pi)$ at $x = -L_\pi$, i.e.

$$\frac{2\Lambda_1(0)}{\sqrt{\pi}} = -\frac{2\tilde{B}}{\sqrt{\pi}} + \mathcal{O}(\sqrt{\gamma}), \quad \frac{2\Lambda_1(0) - \pi}{\sqrt{\pi}} = \frac{2\tilde{B}}{\sqrt{\pi}} + \mathcal{O}(\sqrt{\gamma}).$$

Note that \tilde{A} does not appear in these equations; as a consequence, $\psi_{\text{appr}}^1(x)$ and $\psi_{\text{appr}}^2(x)$ can only be matched for a special value of Λ_1 , $\Lambda_1(0) = \frac{1}{4}\pi$, with $\tilde{B} = -\Lambda_1(0) < 0$. Thus for this special value of Λ_1 and for $\tilde{A} > 0$, we have found a positive C^1 -continuation of the solution $\psi(x)$ of the eigenvalue problem for $\mathcal{L}^3(x; \gamma)$ – recall that $x < 0$ in the domain of $\tilde{\psi}(x)$. At the point of discontinuity ($-x_1$ for $\tilde{\psi}(x)$, or at $x = 0$ in the original coordinates of (3.1)), we have

$$(3.26) \quad \begin{aligned} \psi_{\text{appr}}^2(-x_1) &= \gamma\tilde{\psi}(-x_1) = \gamma\left[\frac{1}{2}\sqrt{2}\tilde{A} - \frac{\pi}{8}\sqrt{2}(\ln(\sqrt{2}-1) - \sqrt{2})\right] + \mathcal{O}(\gamma^2), \\ \frac{d}{dx}\psi_{\text{appr}}^2(-x_1) &= \gamma\frac{d}{dx}\tilde{\psi}(-x_1) = \gamma\left[\frac{1}{2}\tilde{A} - \frac{\pi}{8}(\ln(\sqrt{2}-1) + 3\sqrt{2})\right] + \mathcal{O}(\gamma^2). \end{aligned}$$

Hence, we have constructed for a special choice of Λ , $\Lambda = \Lambda_* = \frac{\pi}{4}\gamma + \mathcal{O}(\gamma\sqrt{\gamma}) > 0$, an approximation of a family of positive solutions of the eigenvalue problem for $\mathcal{L}^3(x; \gamma)$ on $x < 0$ – in the coordinates of (3.1) – that attain the values given by (3.26) at $x = 0$, and that decay to 0 as $x \rightarrow -\infty$. The question is now whether we can ‘glue’ an element of this family in a C^1 -fashion to a solution of the eigenvalue problem for $\mathcal{L}^3(x; \gamma)$ on $x > 0$ – with $\Lambda = \Lambda_*$ – that decays (exponentially) as $x \rightarrow \infty$. If that is

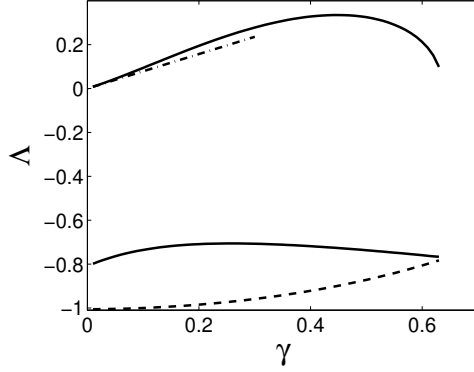


FIG. 3.4. The eigenvalues of the the linear operator associated to the type 3 semifluxon as a function of the bias current γ . The result that the largest eigenvalue is always positive shows the instability of type 3 semifluxon. When $\gamma \ll 1$, according to (3.29) the largest eigenvalue is approximated by $\Lambda = \frac{\pi}{4}\gamma$ shown in dash-dotted line. The dashed line is the boundary of the continuous spectrum.

possible, we have constructed a positive integrable solution to the eigenvalue problem for $\mathcal{L}^3(x; \gamma)$, which implies that $\Lambda_* > 0$ is the critical eigenvalue and that $\phi_\pi^3(x)$ is unstable.

An approximation of $\psi(x)$ on $x > 0$, $\psi_{\text{appr}}^3(x)$, is obtained by linearizing along $\phi_{\text{appr}}^3(x)$ and by translating x so that $x \in (x_1, \infty)$. Since $\psi_{\text{appr}}^3(x)$ has to match to expressions of $\mathcal{O}(\gamma)$ (3.26) at x_1 , we also scale $\psi_{\text{appr}}^3(x)$, $\psi_{\text{appr}}^3(x) = \gamma \hat{\psi}(x)$. We find that $\mathcal{L}\hat{\psi} = \mathcal{O}(\gamma)$ so that $\hat{\psi}(x)$ again has to be (at leading order) a linear combination of $\psi_b(x)$ and $\psi_u(x)$ (3.16). However, $\hat{\psi}$ must be bounded as $x \rightarrow \infty$, which yields that $\hat{\psi}(x) = \hat{A}/\cosh x + \mathcal{O}(\gamma)$ for some $\hat{A} \in \mathbb{R}$. At the point of discontinuity we thus have

$$(3.27) \quad \begin{aligned} \psi_{\text{appr}}^3(x_1) &= \gamma \hat{\psi}(x_1) = \frac{1}{2}\sqrt{2}\hat{A}\gamma + \mathcal{O}(\gamma^2), \\ \frac{d}{dx}\psi_{\text{appr}}^3(x_1) &= \gamma \frac{d}{dx}\hat{\psi}(x_1) = -\frac{1}{2}\hat{A}\gamma + \mathcal{O}(\gamma^2). \end{aligned}$$

A positive C^1 -solution of the eigenvalue problem for $\mathcal{L}^3(x; \gamma)$ exists (for $\Lambda = \Lambda_*$) if there exist $\tilde{A}, \hat{A} > 0$ such that (see (3.26) and (3.27))

$$(3.28) \quad \begin{aligned} \frac{1}{2}\sqrt{2}\tilde{A} - \frac{\pi}{8}\sqrt{2}(\ln(\sqrt{2}-1) - \sqrt{2}) &= \frac{1}{2}\sqrt{2}\hat{A} \\ \frac{1}{2}\tilde{A} - \frac{\pi}{8}(\ln(\sqrt{2}-1) + 3\sqrt{2}) &= -\frac{1}{2}\hat{A} \end{aligned}$$

Since the solution of this system is given by $\tilde{A} = \frac{1}{4}\pi[\sqrt{2} + \ln(\sqrt{2}-1)] > 0$ and $\hat{A} = \frac{1}{2}\pi\sqrt{2} > 0$, we conclude that the eigenvalue problem for the π -fluxon $\phi_\pi^3(x; \gamma)$ has a positive largest eigenvalue

$$(3.29) \quad \Lambda_* = \frac{\pi}{4}\gamma + \mathcal{O}(\gamma\sqrt{\gamma}).$$

Hence the eigenvalue for γ small is positive. From Lemma 3.3 it follows that there are no zero eigenvalues between 0 and γ_{cr} , hence the largest eigenvalue of $\mathcal{L}^3(\gamma)$ is positive for all values of γ . \square

REMARK 3.10. For any $\lambda = \mathcal{O}(\sqrt{\gamma})$, or equivalently any $\Lambda_1 = \mathcal{O}(1)$, there exists a (normalized) solution to the eigenvalue problem for $\mathcal{L}^3(x; \gamma)$ on $x < 0$ that decays

as $x \rightarrow -\infty$, and that is approximated by $\psi_{\text{appr}}^1(x)$ and $\psi_{\text{appr}}^2(x)$ (matched in a C^1 -fashion at $\pm L_\pi$). If Λ_1 is not $\mathcal{O}(\sqrt{\gamma})$ close to $\frac{1}{4}\pi$, however, $\psi_{\text{appr}}^2(x)$ cannot be scaled as $\gamma\tilde{\psi}(x)$ and the solution is not $\mathcal{O}(\gamma)$ at the point of discontinuity – in general it is $\mathcal{O}(1)$. Moreover, for any $\Lambda_1 = \mathcal{O}(1)$, there also exists on $x > 0$ a 1-parameter family of (non-normalized) eigenfunctions for the eigenvalue problem for $\mathcal{L}^3(x; \gamma)$ that decay as $x \rightarrow \infty$. In this family there is one unique solution that connects continuously to the (normalized) solution at $x < 0$. In fact, one could define the jump in the derivative at $x = 0$, $\mathcal{J}(\lambda; \gamma)$, as an Evans function expression (note that $\mathcal{J}(\lambda; \gamma)$ can be computed explicitly at $\gamma = 0$, see [10]). By definition, λ^2 is an eigenfunction of $\mathcal{L}^3(x; \gamma)$ if and only if $\mathcal{J}(\lambda; \gamma) = 0$. In the above analysis we have shown that $\mathcal{J}(\lambda_*; \gamma) = 0$ for $\lambda_* = \frac{1}{2}\sqrt{\pi\gamma} + \mathcal{O}(\gamma)$.

REMARK 3.11. The classical, driven, sine-Gordon equation, i.e. $\theta \equiv 0$ and $\gamma \neq 0$ in (3.1), has a standing pulse solution, that can be seen, especially for $0 < \gamma \ll 1$, as a fluxon/anti-fluxon pair. This solution is approximated for $\frac{d}{dx}\phi > 0$ (the fluxon) by $\phi_{\text{appr}}^1(x)$ and for $\frac{d}{dx}\phi < 0$ (the anti-fluxon) by $\phi_{\text{appr}}^1(-x)$. It is (of course) unstable, the (approximation of the) critical unstable eigenvalue can be obtained from (3.24). The corresponding eigenfunction is approximated by $\psi_{\text{appr}}^1(x)$ on $(-\infty, L_\pi)$, and we conclude from (3.24) that $\frac{d}{dx}\psi_{\text{appr}}^1(L_\pi) = 0$ for $\lambda^2 = \gamma\Lambda_1 = \gamma\frac{\pi}{2} + \mathcal{O}(\gamma\sqrt{\gamma})$ (while $\psi_{\text{appr}}^1(L_\pi) > 0$). Hence, for this value of Λ_1 , we can match $\psi_{\text{appr}}^1(x)$ to $\psi_{\text{appr}}^2(x) = \psi_{\text{appr}}^1(-x)$ in a C^1 -fashion, it gives a uniform $\mathcal{O}(\gamma)$ -approximation of the critical, positive (even, ‘two-hump’) eigenfunction of the fluxon/anti-fluxon pair at the eigenvalue $\lambda_+ = \frac{1}{2}\sqrt{2\pi}\sqrt{\gamma} + \mathcal{O}(\gamma) > 0$.

To consider the relation between the eigenvalues of $\mathcal{L}^3(x; \gamma)$ and the stability problem of $\phi_\pi^3(x; \gamma)$, we denote the largest eigenvalue of $\mathcal{L}^3(x; \gamma)$ by $\Lambda^3(\gamma)$. The associated eigenvalues for the linearizations are solution of the equation $\lambda^2 - \Lambda^3(\gamma) = 0$, hence $\lambda = \pm\sqrt{\Lambda^3(\gamma)}$. Since $\Lambda^3(\gamma) > 0$, this implies that one of the two eigenvalues has positive real part, hence the fluxons of type 3 are unstable. In Fig. 3.4, we present numerical calculations of the eigenvalues of type 3 semifluxon as a function of the bias current γ .

REMARK 3.12. A type 3 semifluxon can be seen as a concatenation of a 2π - and a $-\pi$ -kink in the limit $\gamma \rightarrow 0$. In that limit the other eigenvalue of $\mathcal{L}^3(x; \gamma)$ converges to $-\frac{1}{4}(\sqrt{5} + 1)$ (Figure 3.4) which is a contribution of the $-\pi$ -kink.

4. Lattice π -kinks and their spectra in the continuum limit. In this section, we consider (2.9) for a small lattice spacing a , i.e., the driven 0 - π sine-Gordon equation with a small perturbation due to lattice spacing effects. For $a = 0$, the semifluxons of all types are constructed as heteroclinic connections with transversal intersections at $x = 0$ in the two-dimensional phase space of the static equation (2.10). Therefore, all three types of semifluxons will still exist in the perturbed system with $0 < a \ll 1$, see [11]. The three types of semifluxons are denoted as $\phi_\pi^i(x; a; \gamma)$, for $i = 1, 2$ and 3 . In Fig. 4.1, we present the phase portraits of the sine-Gordon equation both with and without the effect of a perturbation due to lattice spacing.

The lattice spacing a does not affect the stationary points of the phase portraits, as can be easily checked. The existence parameters γ^* and γ_{cr} will be influenced by the lattice spacing a . For a small, they are

$$(4.1) \quad \gamma^*(a) = \frac{2}{\sqrt{4 + \pi^2}} + \underbrace{\frac{2\pi}{3(\pi^2 + 4)^2}}_{\approx 0.0109} a^2 + \mathcal{O}(a^4),$$

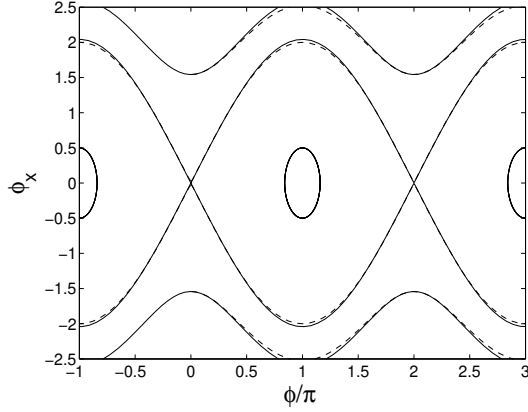


FIG. 4.1. The phase portrait of the stationary system (2.10) for $\gamma = 0$ and some values of the lattice spacing a . The dashed lines are the unperturbed phase portrait for $a = 0$ and the other lines correspond to $a = 0.5$.

$$(4.2) \quad \gamma_{\text{cr}}(a) = \frac{2}{\pi} + \underbrace{\frac{\sqrt{\pi^2 - 4} - \pi + 2 \arcsin(\frac{2}{\pi})}{3\pi^2}}_{\approx 0.0223} a^2 + \mathcal{O}(a^4),$$

see [31] for details. For $\gamma > \gamma_{\text{cr}}(a)$ no static semifluxon exists.

As we have seen in the last section, for $a = 0$, the type 3 semifluxon is marginally unstable at $\gamma = \gamma_{\text{cr}}$ and γ near zero. So there is a possibility that lattice spacing effects stabilize the type 3 semifluxon near those values of γ . However, it turns out that this is not the case and the stability of the semifluxons is similar to the case $a = 0$.

THEOREM 4.1. *For a small, the linearizations about the π -kinks have the following properties:*

(i) *The eigenvalues of the linearization about the monotonic type 1 π -kink $\phi_\pi^1(x; a; \gamma)$ are strictly negative for $0 \leq \gamma < \gamma_{\text{cr}}(a)$. At $\gamma = \gamma_{\text{cr}}(a)$, the largest eigenvalue is zero. These π -kinks are linearly stable.*

(ii) *The largest eigenvalue of the linearization about the monotonic type 2 π -kink $\phi_\pi^2(x; a; \gamma)$ is strictly positive for $0 < \gamma < \gamma^*(a)$. These π -kinks are linearly unstable.*

(iii) *The largest eigenvalue of the linearization about the monotonic type 3 π -kink $\phi_\pi^3(x; a; \gamma)$ is strictly positive for $0 < \gamma < \gamma_{\text{cr}}(a)$. These π -kinks are linearly unstable. In the limit for $\gamma \rightarrow 0$ and $\gamma \rightarrow \gamma_{\text{cr}}(a)$, the largest eigenvalue converges to zero.*

The proof of this theorem will proceed along similar lines as the proof in the previous section. First we consider the eigenvalue problem of a solution $\phi_\pi^i(x; a; \gamma)$, which can be written as

$$\mathcal{L}^i(x; a; \gamma) v = \lambda^2 v,$$

where $\mathcal{L}^i(x; a; \gamma)$ is now defined as the linearization associated with (2.10), i.e.,

$$\begin{aligned} \mathcal{L}^i(x; a; \gamma) &= D_{xx} - \cos(\phi_\pi^i(x; a; \gamma) + \theta(x)) \\ &\quad - \frac{a^2}{12} \left[2 \cos \tilde{\phi} D_{xx} - 2(\phi_\pi^i(x; 0; \gamma))_x \sin \tilde{\phi} D_x \right. \\ &\quad \left. - 1 + 2\gamma \sin \tilde{\phi} - ((\phi_\pi^i(x; 0; \gamma))_x)^2 \cos \tilde{\phi} \right] + \mathcal{O}(a^4) \end{aligned}$$

where $\tilde{\phi} = \phi_\pi^i(x; 0; \gamma) + \theta(x)$.

Lemma 3.3 can be extended to $a \neq 0$ and give a necessary and sufficient condition for $\mathcal{L}^i(x; a; \gamma)$ to have an eigenvalue $\Lambda = 0$.

LEMMA 4.2. *The eigenvalue problem*

$$\mathcal{L}^i(x; \gamma)v = \Lambda v, \quad x \in \mathbb{R},$$

has an eigenvalue $\Lambda = 0$ if and only if one of the following two conditions holds

(i) $D_{xx}\phi_\pi^i(x; a; \gamma)$ is continuous at $x = 0$, i.e., $\phi_\pi^i(0; a; \gamma) = k\pi - a^2 \frac{\gamma}{12} + \mathcal{O}(a^4)$, for some $k \in \mathbb{Z}$;

(ii) $D_x\phi_\pi^i(0; a; \gamma) = 0$ and there are some x_\pm , with $\text{sgn}(x_\pm) = \pm 1$, such that $D_x\phi_\pi^i(x_\pm; a; \gamma) \neq 0$.

Proof. As the proof of Lemma 3.3 is based on the fact that the derivative of the semifluxon is a solution of the linearized system for $x \neq 0$, we can follow the same arguments to prove this lemma. Again this leads to two conditions that either ϕ_{xx}^i is continuous at $x = 0$ or the second condition as stated above.

In order to determine when ϕ_{xx}^i is continuous, we use the static equation (2.10) and expand near $a = 0$:

$$\begin{aligned} D_{xx}\phi_\pi^i(x; a; \gamma) &= (\sin(\phi_\pi^i(x; a; \gamma) + \theta(x)) - \gamma) \left(1 - \frac{a^2}{12} \cos \tilde{\phi}\right) \\ &\quad + \frac{a^2}{6} \sin \tilde{\phi} \left(\gamma \arcsin \gamma + \sqrt{1 - \gamma^2} - \gamma \tilde{\phi} - \cos \tilde{\phi}\right) + \mathcal{O}(a^4). \end{aligned}$$

again with $\tilde{\phi} = \phi_\pi^i(x; 0; \gamma) + \theta(x)$. The continuity of $D_{xx}\phi_\pi^i$ at $x = 0$ leads to the expression for $\phi_\pi^i(x; a; \gamma)$ as given above. \square

At $\gamma = \gamma_{\text{cr}}(a)$, the stable manifold of the $\pi + \arcsin \gamma$ and the homoclinic connection at $\arcsin \gamma$ are tangent, implying that $D_{xx}\phi_\pi^i(x; a; \gamma)$ is continuous at $x = 0$. Thus the first condition of the lemma is satisfied at $\gamma = \gamma_{\text{cr}}(a)$ for $i = 1, 3$. For the same reasons as before, the second condition is never satisfied.

Since $\Lambda = 0$ is an eigenvalue of the linearized operator $\mathcal{L}^i(x; a; \gamma)$ if and only if $\gamma = \gamma_{\text{cr}}(a)$, the sign of the eigenvalues of $\mathcal{L}^i(x; a; \gamma)$ will not change. Thus the behavior of the eigenvalues near $\gamma = 0$ will again determine the stability of the semifluxons.

For $\gamma = 0$ and $\theta = 0$, the sine-Gordon equation with a perturbation due to the lattice spacing has a heteroclinic orbit connecting 0 and 2π . As before, the heteroclinic orbit will play an important role in determining the stability of the semifluxons for small values of γ . For small values of the lattice spacing a , we can approximate this heteroclinic orbit up to order a^2 by using the 2π -fluxon ϕ_{flux} and its linearization.

LEMMA 4.3. *Let $\phi_{\text{flux}}^a(x)$ denote the heteroclinic orbit of the sine-Gordon equation with a perturbation due to the lattice spacing (i.e., (2.9) with $\theta \equiv 0$ and $\gamma = 0$). For the lattice spacing a small, we have for the symmetric (i.e., $\phi_{\text{flux}}^a(0) = \pi$) heteroclinic connection $\phi_{\text{flux}}^a(x)$*

$$(4.3) \quad \phi_{\text{flux}}^a(x) = \phi_{\text{flux}}(x) + a^2 \phi_a(x) + \mathcal{O}(a^4),$$

where

$$(4.4) \quad \phi_a(x) = -\frac{1}{12} \frac{-3 \sinh x + x \cosh x}{\cosh^2 x}.$$

This approximation is valid, uniform in $x \in \mathbb{R}$.

Proof. The spatially localized correction to the kink shape $\phi_{\text{flux}}(x)$ due to the perturbation term representing lattice spacing is sought in the form of perturbation series:

$$\phi_{\text{flux}}^a(x) = \phi_{\text{flux}}(x) + a^2 \phi_a(x) + \mathcal{O}(a^4).$$

It is a direct consequence that $\phi_a(x)$ satisfies

$$(4.5) \quad \mathcal{L}^1(x; 0)\phi_a(x) = f(x) = -\frac{1}{12} \left[2 \cos \phi_{\text{flux}}(x) \partial_{xx} \phi_{\text{flux}}(x) - \sin \phi_{\text{flux}}(x) (\partial_x \phi_{\text{flux}}(x))^2 - \cos \phi_{\text{flux}}(x) \sin \phi_{\text{flux}}(x) \right],$$

where $\mathcal{L}^1(x; 0)$ is the linearized operator associated to the fluxon, i.e., $\mathcal{L}^1(x; 0) = D_{xx} - \cos \phi_{\text{flux}}(x)$.

Using the variation of constants method, we obtain the general solution of (4.5), i.e.

$$(4.6) \quad \phi_a(x) = A(x) \operatorname{sech} x + B(x) (x \operatorname{sech} x + \sinh x),$$

where

$$A(x) = A_0 + \frac{1}{24} \left[2 \ln \left(\frac{1 - \cosh x - \sinh x}{\cosh x - 1 - \sinh x} \right) + \frac{6 \sinh x}{\cosh x} - \frac{4 \sinh x}{\cosh^3 x} + \int_0^x \frac{\xi f(\xi)}{\cosh \xi} d\xi \right],$$

$$B(x) = B_0 - \frac{1}{24} \left[2 + \frac{1}{\cosh^2 x} - \frac{3}{\cosh^4 x} \right].$$

The integration constant B_0 is determined by the condition that $\phi_a(x)$ is bounded, leading to $B_0 = \frac{1}{12}$. The integration constant A_0 is determined by the requirement that $\phi_{\text{flux}}^a(0) = \pi$, hence $\phi_a(0) = 0$, giving that $A_0 = 0$. \square

For $\gamma = 0$, the static model (2.10) for a 0 - π Josephson junction with lattice spacing effects has both a π - and a 3π -kink solution. The 2π -heteroclinic orbit found above, can be used to derive approximations for those kinks.

LEMMA 4.4. *For a small and $\gamma = 0$, we have an explicit expression for the π - and 3π -fluxon up to order $\mathcal{O}(a^2)$, respectively:*

$$(4.7) \quad \begin{aligned} \phi_\pi^1(x; a; 0) &= \phi_\pi^1(x; 0) + a^2 \begin{cases} -u_\pi^1(x - \ln(1 + \sqrt{2})), & \text{for } x < 0 \\ u_\pi^1(-x - \ln(1 + \sqrt{2})), & \text{for } x > 0 \end{cases} \\ \phi_{3\pi}^2(x; a; 0) &= \phi_{3\pi}^2(x; 0) + a^2 \begin{cases} -u_{3\pi}^1(x + \ln(1 + \sqrt{2})), & \text{for } x < 0 \\ u_{3\pi}^1(-x + \ln(1 + \sqrt{2})), & \text{for } x > 0 \end{cases} \end{aligned}$$

where $\phi_\pi^1(x; 0)$ and $\phi_{3\pi}^2(x; 0)$ are the π - resp. the 3π - fluxons as defined in (3.11) and

$$u_\pi^1(x) = \frac{1}{12 \cosh x} \left(\frac{3\sqrt{2}}{2} - \frac{1}{2} \ln(3 - \sqrt{2}) + 3 \tanh x - x \right)$$

$$u_{3\pi}^1(x) = \frac{1}{12 \cosh x} \left(-\frac{3\sqrt{2}}{2} + \frac{1}{2} \ln(3 - \sqrt{2}) + 3 \tanh x - x \right).$$

4.1. Stability of type 1 semifluxon. We will show that the type 1 wave $\phi_\pi^1(x; a; \gamma)$ is linearly stable for small a and $0 \leq \gamma \leq \gamma_{\text{cr}}$ by analyzing the largest eigenvalue of $\mathcal{L}^1(x; a; \gamma)$ for $0 \leq \gamma \leq \gamma_{\text{cr}}(a)$.

LEMMA 4.5. *For the lattice spacing parameter a sufficiently small and $0 \leq \gamma < \gamma_{\text{cr}}(a)$, the largest eigenvalue of $\mathcal{L}^1(x; a; \gamma)$ is strictly negative. For $\gamma = \gamma_{\text{cr}}(a)$, the operator $\mathcal{L}^1(x; a; \gamma_{\text{cr}}(a))$ has 0 as its largest eigenvalue. For $\gamma = 0$, the largest eigenvalue decreases as a increases and is proportional to $-\frac{1}{4}(\sqrt{5} + 1) - 0.0652a^2 + \mathcal{O}(a^4)$.*

Proof. First we look at the stability of the π -kink at $\gamma = 0$. Writing $v(x) = v^0(x) + a^2 v^1(x) + \mathcal{O}(a^4)$ and $\Lambda = \Lambda_0 + a^2 \Lambda_1 + \mathcal{O}(a^4)$ and expanding the eigenvalue

problem for the stability of the π -kink $\phi_\pi^1(x; a; 0)$ in a Taylor series, result in the following equations

$$(4.8) \quad \begin{aligned} (\mathcal{L}^1(x; 0; 0) - \Lambda_0) v^0(x) &= 0, \\ (\mathcal{L}^1(x; 0; 0) - \Lambda_0) v^1(x) &= (\Lambda_1 - u_\pi^1(x) \sin(\phi_\pi^1(x; 0) + \theta)) v^0(x) - g(x), \end{aligned}$$

where $\mu = \sqrt{\Lambda_0 + 1}$, $\Lambda_0 = -\frac{1}{4}(\sqrt{5} + 1)$,

$$\begin{aligned} v^0(x) &= \begin{cases} e^{\mu(x - \ln(1 + \sqrt{2}))} [\tanh(x - \ln(1 + \sqrt{2})) - \mu], & \text{for } x < 0, \\ e^{\mu(-x - \ln(1 + \sqrt{2}))} [\tanh(-x - \ln(1 + \sqrt{2})) - \mu], & \text{for } x > 0, \end{cases} \\ g(x) &= \frac{1}{12} \left[2v_{xx}^0 \Lambda_0 + v^0 + 2v_{xx}^0 \cos \tilde{\phi}(x) - 2 \cos^2 \tilde{\phi}(x) v^0 - 2\partial_{xx}(\phi_\pi^1(x; 0)) \sin \tilde{\phi}(x) v^0 \right. \\ &\quad \left. - 2\partial_x \phi_\pi^1(x; 0) \sin \tilde{\phi}(x) v_x^0 - (\partial_x \phi_\pi^1(x; 0))^2 \cos \tilde{\phi}(x) v^0 - v^0 \Lambda_0^2 - 2v^0 \Lambda_0 \cos \tilde{\phi}(x) \right], \end{aligned}$$

with again $\tilde{\phi}(x) = \phi_\pi^1(x; 0) + \theta(x)$ (see Lemma 3.5).

The parameter value of Λ_1 is calculated by solving (4.8) for a bounded and decaying solution $v^1(x)$. The general solution can be derived by using the variation of constant method because we have the homogeneous solutions of the equation. One can also use the Fredholm theorem (see, e.g., [30]), i.e. the sufficient and necessary condition for (4.8) to have a solution $v^1 \in H_2(\mathbb{R})$ is that the inhomogeneity is perpendicular to the null space of the self-adjoint operator of $\mathcal{L}^1(x; 0; 0)$. If $\langle \cdot, \cdot \rangle$ denotes an inner product in $H_2(\mathbb{R})$, then this condition gives

$$0 = \langle (\mathcal{L}^1(x; 0; 0) - \Lambda_0) v^1, v^0 \rangle = \langle \Lambda_1 v^0 - u_\pi^1 v^0 \sin(\phi_\pi^1(x; 0) + \theta) - g, v^0 \rangle$$

which implies that

$$(4.9) \quad \Lambda_1 = \frac{3584(70\sqrt{2}(1 + \sqrt{5}) - 99(1 + \sqrt{5}))}{24576(-70\sqrt{10} - 350\sqrt{2} + 495 + 99\sqrt{5})} \approx -0.0652.$$

Now assume that the operator $\mathcal{L}^1(x; \gamma)$ has a positive eigenvalue $\Lambda^1(\gamma)$ for some $0 \leq \gamma < \gamma_{\text{cr}}(a)$. Since Λ depends continuously on γ , there has to be some $0 < \hat{\gamma} < \gamma_{\text{cr}}(a)$ such that $\Lambda^1(\hat{\gamma}) = 0$. However, from Lemma 4.2 it follows that this is not possible. \square

4.2. Instability of type 2 semifluxon. In Lemma 3.6 we have seen that for $a = 0$, the linearization about the type 2 semifluxon has a strictly positive largest eigenvalue. Also the limits of this eigenvalue for $\gamma \rightarrow 0$ and $\gamma \rightarrow \gamma^*$ are still strictly positive. Thus a small perturbation associated with the lattice spacing can not stabilize the type 2 semifluxons.

For completeness, we will consider the case $\gamma = 0$. In this limit, the type 2 semifluxon can be seen as a concatenation of a 3π -kink and a -2π -kink. As before, the limit of the largest eigenvalue for $\gamma \rightarrow 0$ will be equal to the largest eigenvalue of the 3π -kink. We have seen that the largest eigenvalue of the 3π -kink at $\gamma = 0$ and $a = 0$ is strictly positive and the following lemma shows that small lattice spacing effects increase this eigenvalue.

LEMMA 4.6. *For the lattice spacing parameter a sufficiently small, the largest eigenvalue of the linearization $\mathcal{L}^2(x; a; 0)$ about the 3π -kink $\phi_{3\pi}^2(x; a; 0)$ is strictly positive. Moreover, it increases as a increases and is proportional to $\frac{1}{4}(\sqrt{5} - 1) + 0.0652a^2 + \mathcal{O}(a^4)$.*

Proof. Note that the lowest order analytic expressions for the π - and the 3π -kink differs only in the sign of the 'kink-shift' (see (4.7)). Because of this, we can follow the same steps as the proof of Lemma 4.5. Writing the largest eigenvalue of a 3π -kink as $\Lambda = \Lambda_0 + a^2\Lambda_1 + \mathcal{O}(a^4)$, with $\Lambda_0 = (\sqrt{5} - 1)/4$ as has been calculated in Lemma 3.6, we compute Λ_1 to be:

$$(4.10) \quad \Lambda_1 = \frac{3584(665857(\sqrt{5} - 1) - 470832\sqrt{2}(\sqrt{5} + 1))}{24576(3329285 - 2354160\sqrt{2} - 665857\sqrt{5} + 470832\sqrt{10})} \approx 0.0652.$$

□

Thus up to order $\mathcal{O}(a^4)$ the lattice spacing effects destabilize the 3π -kink.

Because a 2π -fluxon in the 'ordinary' sine-Gordon equation can be pinned by lattice spacing effects, one might expect to have a stable 3π -kink in the $0-\pi$ sine-Gordon equation with larger lattice spacing effects. This is confirmed by numerical calculations in section 6, see Figure 6.7. If the 3π -kink is stable for $\gamma = 0$, a stable type 2 semi-kink might exist for $\gamma > 0$ when the repelling force between the 3π -kink and the anti-fluxon is smaller than the energy to move a fluxon along lattices. However, in section 6 it will be shown numerically that the type 2 semikink is unstable for all values of the lattice spacing, see Figure 6.8(b).

4.3. Instability of type 3 semifluxon. For γ small or close to γ_{cr} , it has been shown in Lemma 3.9 that the type 3 semifluxons are weakly unstable. This opens the possibility that the perturbation term representing the lattice spacing stabilizes the semifluxon. This is not the case however.

LEMMA 4.7. *For small lattice spacing a and bias current $0 < \gamma < \gamma_{\text{cr}}(a)$, the largest eigenvalue of the linearization $\mathcal{L}^3(x; a; \gamma)$ about the type 3 semifluxon $\phi_\pi^3(x; a; \gamma)$ is strictly positive. For $\gamma = \gamma_{\text{cr}}(a)$, the operator $\mathcal{L}^3(x; a; \gamma_{\text{cr}})$ has 0 as its largest eigenvalue. For γ near zero and $a^2 = \gamma\hat{a}^2$, the largest eigenvalue of $\mathcal{L}^3(x; a; \gamma)$ is $\Lambda_* = (\frac{\pi}{4} + \frac{7}{180}\hat{a}^2) \gamma + \mathcal{O}(\gamma\sqrt{\gamma})$.*

Proof. At $\gamma = \gamma_{\text{cr}}$, the solution $\phi_\pi^3(x; a; \gamma_{\text{cr}}(a)) = \phi_\pi^1(x; a; \gamma_{\text{cr}}(a))$. Hence from Lemma 4.5 it follows that the largest eigenvalue of the linearization about $\phi_\pi^3(x; a; \gamma_{\text{cr}}(a))$ vanishes.

From Lemma 3.9 it follows that the largest eigenvalue of the linearization about $\phi_\pi^3(x; a; \gamma)$ is positive for $a = 0$ and $0 < \gamma < \gamma_{\text{cr}}$. Thus a small perturbation can not change the positive sign of the largest eigenvalue if γ is not near 0 or γ_{cr} . Now assume that a small perturbation would lead to a negative largest eigenvalue near $\gamma = 0$ or $\gamma = \gamma_{\text{cr}}$. Then there has to be a zero eigenvalue near $\gamma = 0$ or $\gamma = \gamma_{\text{cr}}$, but this is not possible according to Lemma 4.5. Thus we can conclude that the largest eigenvalue is always positive.

To complete the proof, we will derive the asymptotic expression of the eigenvalue near $\gamma = 0$. Since both a and γ are small, we relate those two parameters by writing $a^2 = \gamma\hat{a}^2$. Now the approximation for the type 3 semifluxon can be written as

$$\phi_\pi^3(x; \hat{a}\sqrt{\gamma}; \gamma) = \begin{cases} \phi_{\text{flux}}(\hat{x}) + \gamma\phi_1(\hat{x}) + \gamma\hat{a}^2\phi_a(\hat{x}) + \gamma^2R_2(\hat{x}; \gamma), & x < -L_\pi(\gamma) + x_1, \\ \phi_{\text{flux}}(-\tilde{x}) + \gamma\phi_1(-\tilde{x}) + \gamma\hat{a}^2\phi_a(-\tilde{x}) + \gamma^2R_2(-\tilde{x}; \gamma), & -L_\pi(\gamma) + x_1 < x < 0, \\ \pi + \phi_{\text{flux}}(-x - x_1) + \mathcal{O}(\gamma), & x > 0, \end{cases}$$

where $\hat{x} = x - x_1 + 2L_\pi(\gamma)$ and $\tilde{x} = x - x_1$. It can be shown that the shift $L_\pi(\gamma)$ does not depend on \hat{a}^2 in lowest order, i.e., $L_\pi(\gamma) = \frac{1}{2}|\ln \gamma| + \ln \frac{4}{\sqrt{\pi}} + \mathcal{O}(\sqrt{\gamma})$.

To find largest eigenvalue, we set again $\Lambda^3(\gamma) = \gamma\Lambda_1(0)$ and follow the steps in the proof of Lemma 3.9 with some additional terms added to some expressions.

First, we consider the part of the approximation with $x < -L_\pi(\gamma) + x_1$ or $\hat{x} < L_\pi(\gamma)$. As before, we drop the hat in \hat{x} in this part of the arguments. On $(-\infty, L_\pi)$, the general solution of the eigenvalue problem of the order $\mathcal{O}(\gamma)$ after expanding $\psi_{\text{approx}}^1 = \psi_0 + \gamma\psi_1$ is

$$\begin{aligned} \psi_1(x) = & \left[\frac{\pi}{4} - \frac{1}{2}\Lambda_1 \left(\ln \cosh x + \int_0^x \frac{\xi}{\cosh^2 \xi} d\xi \right) \right] \frac{1}{\cosh x} \\ & + \left[\frac{1}{2}\Lambda_1(0) + \frac{1}{2}\Lambda_1 \tanh x \right] \left(\frac{x}{\cosh x} + \sinh x \right) + \frac{1}{2} \left(\frac{d}{dx}\phi_1 + \hat{a}^2 \frac{d}{dx}\phi_a \right) \\ & - \frac{e^x}{360(e^{2x} + 1)^3} \left[16 \ln 2 + e^{2x}(32 \ln 2 - 295 + 60x) + 30x + 137 + 7e^{6x} \right. \\ & \quad \left. - 16 \ln(e^{2x} + 1)(e^{2x} + 1)^2 + e^{4x}(151 + 30x + 16 \ln 2) \right]. \end{aligned}$$

We note that the error term $|\psi(x) - \psi_{\text{appr}}^1(x)| = \gamma^2 |S_2(x; \gamma)|$ is still at most $\mathcal{O}(\gamma)$ on $(-\infty, L_\pi)$.

Next consider the second part of the approximation, i.e., x between $-L_\pi(\gamma) + x_1$ and 0 or $\tilde{x} < -L_\pi(\gamma)$. Again, we drop the tilde in \tilde{x} . We scale $\psi(x)$ as $\gamma\tilde{\psi}(x)$. The linearization $\tilde{\psi}(x)$ along $\phi_{\text{appr}}^2(x)$ on the interval $(-L_\pi, -x_1)$ must solve $\mathcal{L}\tilde{\psi} = \mathcal{O}(\gamma)$. Thus, at leading order

$$\tilde{\psi}(x) = \frac{\tilde{A}}{\cosh x} + \tilde{B} \left(\frac{x}{\cosh x} + \sinh x \right).$$

The last part of the approximation of $\psi(x)$ on $x > 0$, $\psi_{\text{appr}}^3(x)$, is obtained by linearizing along $\phi_{\text{appr}}^3(x)$ and by translating x so that $x \in (x_1, \infty)$. We also scale $\psi_{\text{appr}}^3(x) = \gamma\hat{\psi}(x)$. As $\hat{\psi}$ must be bounded for $x \rightarrow \infty$, it follows that $\hat{\psi}(x) = \hat{A}/\cosh x + \mathcal{O}(\gamma)$ for some $\hat{A} \in \mathbb{R}$.

Finally we have to connect all parts of the eigenfunction in a C^1 -fashion. This determines the values of $\Lambda_1(0)$, \tilde{A} , \tilde{B} , and \hat{A} as

$$\Lambda_1(0) = \frac{1}{4}\pi + \frac{7}{180}\hat{a}^2, \quad \tilde{B} = -\Lambda_1(0), \quad \tilde{A} = \frac{1}{4}\pi[\sqrt{2} + \log(\sqrt{2}-1)], \quad \text{and} \quad \hat{A} = \frac{1}{2}\pi\sqrt{2},$$

thus $\Lambda_1(0) > 0$, $\tilde{B} < 0$, $\tilde{A} > 0$ and $\hat{A} > 0$. And we can conclude that the eigenvalue problem for the π -fluxon $\phi_\pi^3(x; \hat{a}\sqrt{\gamma}; \gamma)$ has a positive largest eigenvalue

$$\Lambda_* = \left(\frac{\pi}{4} + \frac{7}{180}\hat{a}^2 \right) \gamma + \mathcal{O}(\gamma\sqrt{\gamma}).$$

□

5. Semikinks in the weak-coupling limit. In this section we will consider the discrete $0-\pi$ sine-Gordon equation (2.3) when the lattice parameter a is large. The time independent version of (2.3) is well-known: when $\gamma = 0$, it corresponds to the so-called Standard or Taylor-Greene-Chirikov map [9] and when $\gamma \neq 0$, it is called the Josephson map [23]. Since we are interested in the case that the lattice spacing a is large, we introduce the coupling parameter ε as $\varepsilon = \frac{1}{a^2}$ and the equation becomes

$$(5.1) \quad \ddot{\phi}_n - \varepsilon [\phi_{n-1} - 2\phi_n + \phi_{n+1}] = -\sin(\phi_n + \theta_n) + \gamma.$$

When there is no coupling, i.e. $\varepsilon = 0$, it can be seen immediately that there are infinitely many steady state solutions:

$$\phi_n = \begin{cases} \cos(k_n\pi) \arcsin \gamma + k_n\pi, & n = 0, -1, -2, \dots \\ \cos(k_n\pi) \arcsin \gamma + (k_n + 1)\pi, & n = 1, 2, 3, \dots, \end{cases}$$

where k_n is an integer. The only monotone semi-kink is the solution with $k_n = 0$ for $n \in \mathbb{Z}$, thus it is natural to identify this semikink with the type 1 semikink. However, it is less clear which solution would correspond to the type 2 and type 3 semi-kinks. Possible candidates for the type 2 wave are solutions for which there is some $N \in \mathbb{N}$ such that $k_n = 0$ for $n \leq 0$ and $n \geq N$ and $k_n = 1$ for $0 < n < N$. Similarly, candidates for the type 3 wave are solutions for which there is some $N \in \mathbb{N}$ such that $k_n = 0$ for $n \leq -N$ and $n \geq 0$ and $k_n = 1$ for $-N < n < 0$. But there are many other candidates involving combinations of $k_n = 0$ or $k_n = 1$ as well. If one starts with such a wave in the uncoupled limit, i.e., with $\varepsilon \ll 1$ or $a \rightarrow \infty$ and uses continuation to follow this wave in the discrete system (5.1) towards $a = 0$ or $\varepsilon \rightarrow \infty$, then it turns out that most waves end in a saddle-node bifurcation. More details about the continuation can be found in section 6.

In this section we will focus on the analytical study of the type 1 semi-kink for the coupling parameter ε small (thus the lattice spacing a large). We will denote this wave by $\Phi_\pi^1(n; \varepsilon; \gamma)$ and for $\varepsilon = 0$, we have

$$\Phi_\pi^1(n; 0; \gamma) = \begin{cases} \arcsin \gamma, & n = 0, -1, -2, \dots \\ \pi + \arcsin \gamma, & n = 1, 2, 3, \dots \end{cases}$$

The existence of the continuation of (5.2) for small coupling ε is guaranteed by the following lemma.

LEMMA 5.1. *The steady state solution $\Phi_\pi^1(n; 0; \gamma)$, representing the semifluxon of type 1 in the uncoupled limit $\varepsilon = 0$, can be continued for ε small and $\gamma < 1$. It is given by*

$$(5.2) \quad \Phi_\pi^1(n; \varepsilon; \gamma) = \begin{cases} \arcsin \gamma + \mathcal{O}(\varepsilon^2), & n \leq -1; \\ \arcsin \gamma + \varepsilon \frac{\pi}{\sqrt{1-\gamma^2}} + \mathcal{O}(\varepsilon^2), & n = 0; \\ \pi + \arcsin \gamma - \varepsilon \frac{\pi}{\sqrt{1-\gamma^2}} + \mathcal{O}(\varepsilon^2), & n = 1; \\ \pi + \arcsin \gamma + \mathcal{O}(\varepsilon^2), & n \geq 2. \end{cases}$$

For γ close to one, we write $\gamma = 1 - \varepsilon\tilde{\gamma}$. If $\tilde{\gamma} > \pi$, then the type 1 solution is:

$$(5.3) \quad \Phi_\pi^1(n; \varepsilon; 1 - \varepsilon\tilde{\gamma}) = \begin{cases} \frac{\pi}{2} - \sqrt{\varepsilon} \sqrt{2\tilde{\gamma}} + \mathcal{O}(\varepsilon), & n \leq -1; \\ \frac{\pi}{2} - \sqrt{\varepsilon} \sqrt{2(\tilde{\gamma} - \pi)} + \mathcal{O}(\varepsilon), & n = 0; \\ \frac{3\pi}{2} - \sqrt{\varepsilon} \sqrt{2(\tilde{\gamma} + \pi)} + \mathcal{O}(\varepsilon), & n = 1; \\ \frac{3\pi}{2} - \sqrt{\varepsilon} \sqrt{2\tilde{\gamma}} + \mathcal{O}(\varepsilon), & n \geq 2; \end{cases}$$

From (5.3) we obtain the critical bias current for the existence of static semifluxon as

$$(5.4) \quad \gamma_{\text{cr}} = 1 - \varepsilon\pi + \mathcal{O}(\varepsilon^2).$$

Proof. The existence proof for $\gamma < 1$ follows from the implicit function theorem as given in [21, Theorem 2.1] or [24, Lemma 2.2].

For the case $\gamma = 1 - \varepsilon\tilde{\gamma}$, the implicit function theorem as presented in the references above can not be applied immediately. However, after some manipulations, the implicit function theorem can be applied again. First we substitute into the steady state equation $\gamma = 1 - \varepsilon\tilde{\gamma}$ and $\Phi = \Phi_0 + \sqrt{\varepsilon}\tilde{\Phi}$, where $\Phi_0(n) = \frac{\pi}{2}$, for $n \leq 0$ and $\Phi_0(n) = \frac{3\pi}{2}$, for $n \geq 1$. This gives the following equations:

$$\begin{aligned} 0 &= \frac{\cos(\sqrt{\varepsilon}\tilde{\Phi}(n))-1}{\varepsilon} + \tilde{\gamma} - \sqrt{\varepsilon}[\tilde{\Phi}(n-1) - 2\tilde{\Phi}(n) + \tilde{\Phi}(n+1)] =: \tilde{F}_n(\tilde{\Phi}, \varepsilon), \quad n \neq 0, 1 \\ 0 &= \frac{\cos(\sqrt{\varepsilon}\tilde{\Phi}(0))-1}{\varepsilon} + \tilde{\gamma} - \sqrt{\varepsilon}[\tilde{\Phi}(-1) - 2\tilde{\Phi}(0) + \tilde{\Phi}(1)] - \pi =: \tilde{F}_0(\tilde{\Phi}, \varepsilon), \quad n = 0 \\ 0 &= \frac{\cos(\sqrt{\varepsilon}\tilde{\Phi}(1))-1}{\varepsilon} + \tilde{\gamma} - \sqrt{\varepsilon}[\tilde{\Phi}(0) - 2\tilde{\Phi}(1) + \tilde{\Phi}(2)] + \pi =: \tilde{F}_1(\tilde{\Phi}, \varepsilon), \quad n = 1 \end{aligned}$$

Using that $\lim_{\varepsilon \rightarrow 0} \frac{\cos(\sqrt{\varepsilon}\tilde{\Phi}(n))-1}{\varepsilon} = -\frac{1}{2}(\tilde{\Phi}(n))^2$, the definitions for \tilde{F} can be smoothly extended to $\varepsilon = 0$ too. The equations for $\varepsilon = 0$ become

$$\tilde{\Phi}^2(n) = 2\tilde{\gamma}, \quad n \neq 0, 1; \quad \tilde{\Phi}^2(0) = 2(\tilde{\gamma} - \pi); \quad \text{and} \quad \tilde{\Phi}^2(1) = 2(\tilde{\gamma} + \pi).$$

For $|n|$ large, wave should be asymptotic to the center point of the temporal dynamics, hence $\tilde{\Phi}(n) = -\sqrt{2\tilde{\gamma}}$ for $|n|$ large. So for $\tilde{\gamma} \geq \pi$, there are two monotone semi-kinks (recall that the full semi-kink is given by $\Phi_0 + \sqrt{\varepsilon}\tilde{\Phi}$):

$$\tilde{\Phi}^\pm(n; 0; \tilde{\gamma}) = \begin{cases} -\sqrt{2\tilde{\gamma}}, & n \leq -1; \\ \pm\sqrt{2(\tilde{\gamma} - \pi)}, & n = 0; \\ -\sqrt{2(\tilde{\gamma} + \pi)}, & n = 1; \\ -\sqrt{2\tilde{\gamma}}, & n \geq 2. \end{cases}$$

Note that the \pm -solutions collide for $\tilde{\gamma} = \pi$. The linearization $D\tilde{F}(\tilde{\Phi}^\pm, 0)$ is invertible for $\tilde{\gamma} > \pi$, hence the implicit function theorem can be applied again and we have the existence of monotone semi-kinks $\Phi_0(n) + \sqrt{\varepsilon}\tilde{\Phi}^\pm(n, \varepsilon, \tilde{\gamma})$. In analogue with the continuum case, the type 1 wave is the one that has the discontinuity at the lowest value of the phase. The critical bias current for the existence of a static lattice semifluxon follows immediately from the arguments above. \square

The two \pm -solutions near γ_{cr} as derived above in the proof are like the type 1 and type 3 semi-fluxons near γ_{cr} in the PDEs studied in the previous two sections. So in analogue to those PDEs, we can define for $\tilde{\gamma} > \pi$

$$\Phi_\pi^1(n; \varepsilon; 1 - \varepsilon\tilde{\gamma}) = \Phi_0(n) + \sqrt{\varepsilon}\tilde{\Phi}^-(n; \varepsilon; \tilde{\gamma}) \quad \text{and} \quad \Phi_\pi^3(n; \varepsilon; 1 - \varepsilon\tilde{\gamma}) = \Phi_0(n) + \sqrt{\varepsilon}\tilde{\Phi}^+(n; \varepsilon; \tilde{\gamma}).$$

where Φ_0 and $\tilde{\Phi}^\pm$ are as in the proof above. Thus we get

$$(5.5) \quad \Phi_\pi^{1/3}(n; \varepsilon; 1 - \varepsilon\tilde{\gamma}) = \begin{cases} \frac{\pi}{2} - \sqrt{\varepsilon}\sqrt{2\tilde{\gamma}} + \mathcal{O}(\varepsilon), & n \geq -1; \\ \frac{\pi}{2} \mp \sqrt{\varepsilon}\sqrt{2(\tilde{\gamma} - \pi)} + \mathcal{O}(\varepsilon), & n = 0; \\ \frac{3\pi}{2} - \sqrt{\varepsilon}\sqrt{2(\tilde{\gamma} + \pi)} + \mathcal{O}(\varepsilon), & n = 1; \\ \frac{3\pi}{2} - \sqrt{\varepsilon}\sqrt{2\tilde{\gamma}} + \mathcal{O}(\varepsilon), & n \geq 2; \end{cases}$$

The spectral stability of $\Phi_\pi^i(n; \varepsilon; \gamma)$ is obtained by substituting $\phi_n = \Phi_\pi^i(n; \varepsilon; \gamma) + v_n e^{\lambda t}$ in the model equation (2.3). Disregarding the higher order terms in v_n gives the following eigenvalue problem

$$(5.6) \quad L^i(\varepsilon; \gamma)\nu = \Lambda\nu,$$

Combining (5.9), (5.10) and (5.11) shows that there are two possible value for \hat{c} , being $\hat{c}_{\pm} = -\frac{\pi\gamma}{\sqrt{1-\gamma^2}} \pm \frac{\sqrt{1+(\pi^2-1)\gamma^2}}{\sqrt{1-\gamma^2}} + \mathcal{O}(\varepsilon)$ and leads to the eigenvalue Λ and the decay exponent ℓ as a function of ε and γ , i.e.

$$(5.12) \quad \ell_{\pm} = \pm \frac{\sqrt{1-\gamma^2}}{\sqrt{1+(\pi^2-1)\gamma^2}} + \mathcal{O}(\varepsilon),$$

$$(5.13) \quad \Lambda_{\pm} = -\sqrt{1-\gamma^2} + \frac{\varepsilon}{\ell_{\pm}} (\ell_{\pm} - 1)^2 + \mathcal{O}(\varepsilon^2).$$

General Sturm-Liouville theory states that a critical eigenfunction that corresponds to the largest eigenvalue of a continuous eigenvalue problem does not vanish, except probably at $x \rightarrow \pm\infty$. This theorem can also be extended to a discrete eigenvalue problem such that the most critical eigenvector does not have sign changes [1]. Thus, if we have a solution of the form (5.8) with $\ell > 0$, then it is the critical eigenvector.

From (5.12), we see that $\ell_+ > 0$, thus the largest eigenvalue Λ_+ from (5.13) is in the gap between zero and the interval associated with the continuous spectrum, i.e. $\Lambda_+ < 0$. \square

REMARK 5.3. From the details in the proof, note that weak coupling with strong bias current leads to one additional eigenvalue associated with ℓ_- , where $\ell_- < 0$ and $|\ell_-| < 1$. This indicates that the eigenvector of the form (5.8) is localized but has out of phase configuration, i.e. has infinitely many sign changes. This is a typical characteristic of a 'high-frequency' eigenvalue which is confirmed by the fact that Λ_- is indeed smaller than the phonon band. The presence of a high-frequency eigenvalue of a kink was previously reported by Braun, Kivshar, and Peyrard [6] in their study on the Frenkel-Kontorova model with the Peyrard-Remoissenet potential [26].

For γ close to 1, i.e. $\gamma = 1 - \varepsilon\tilde{\gamma}$, with $\tilde{\gamma} > \pi$, both the type 1 and the type 3 wave as given in (5.5) can be analyzed. In the following lemma we also show that both types have a high-frequency eigenvalue.

LEMMA 5.4. *For $\gamma = 1 - \varepsilon\tilde{\gamma}$, with $\tilde{\gamma} > \pi$, the largest eigenvalue of the operator $L^1(\varepsilon; 1 - \varepsilon\tilde{\gamma})$ is strictly negative and the largest eigenvalue of the operator $L^3(\varepsilon; 1 - \varepsilon\tilde{\gamma})$ is strictly positive.*

Proof. As before, we write for an eigenfunction

$$v_n = \begin{cases} cl^{-n}, & n \leq 0, \\ \hat{c}cl^{n-1}, & n \geq 1, \end{cases}$$

for some c , \hat{c} and $|\ell| < 1$ and we substitute this in the eigenvalue problem, which leads to the equations

$$(5.14) \quad \Lambda = -\sin\left(\sqrt{\varepsilon 2\tilde{\gamma}} + \mathcal{O}(\varepsilon)\right) + \varepsilon(1/\ell - 2 + \ell);$$

$$(5.15) \quad \Lambda = \mp \sin\left(\sqrt{2\varepsilon(\tilde{\gamma} - \pi)} + \mathcal{O}(\varepsilon)\right) + \varepsilon(\ell - 2 + \hat{c});$$

$$(5.16) \quad \Lambda = -\sin\left(\sqrt{2\varepsilon(\tilde{\gamma} + \pi)} + \mathcal{O}(\varepsilon)\right) + \varepsilon(\ell - 2 + 1/\hat{c}).$$

where \mp -sign in the second equation is a minus sign for the eigenvalue problem associated with the type 1 wave and the other sign in case of the type 3 wave. Again, by subtracting (5.16) from (5.15), we get a quadratic equation for \hat{c} , with two solutions,

one of order $\frac{1}{\sqrt{\varepsilon}}$ and one of order $\sqrt{\varepsilon}$ (which is easiest found by writing the equation as a quadratic equation for $\frac{1}{\varepsilon}$):

$$\begin{aligned}\frac{1}{\hat{c}_1} &= \frac{1}{\sqrt{\varepsilon}} \left(\sqrt{2(\tilde{\gamma} + \pi)} \mp \sqrt{2(\tilde{\gamma} - \pi)} + \mathcal{O}(\sqrt{\varepsilon}) \right); \\ \hat{c}_2 &= \frac{1}{\sqrt{\varepsilon}} \left(-\sqrt{2(\tilde{\gamma} + \pi)} \pm \sqrt{2(\tilde{\gamma} - \pi)} + \mathcal{O}(\sqrt{\varepsilon}) \right).\end{aligned}$$

Combining (5.14) and (5.15) resp. (5.16) and using the two expressions above gives that in both cases ℓ is of order $\sqrt{\varepsilon}$ and given by

$$\begin{aligned}\frac{1}{\ell_1} &= \frac{1}{\sqrt{\varepsilon}} \left(\sqrt{2\tilde{\gamma}} \mp \sqrt{2(\tilde{\gamma} - \pi)} + \mathcal{O}(\sqrt{\varepsilon}) \right); \\ \frac{1}{\ell_2} &= \frac{1}{\sqrt{\varepsilon}} \left(\sqrt{2\tilde{\gamma}} - \sqrt{2(\tilde{\gamma} + \pi)} + \mathcal{O}(\sqrt{\varepsilon}) \right).\end{aligned}$$

Finally, substitution into (5.14) shows that

$$(5.17) \quad \begin{aligned}\Lambda_1 &= \mp \sqrt{\varepsilon} \sqrt{2(\tilde{\gamma} - \pi)} + \mathcal{O}(\varepsilon); \\ \Lambda_2 &= -\sqrt{\varepsilon} \sqrt{2(\tilde{\gamma} + \pi)} + \mathcal{O}(\varepsilon).\end{aligned}$$

The eigenvalue that corresponds to $\ell > 0$ is Λ_1 .

So clearly the largest eigenvalue Λ_1 is negative in case of the type 1 wave and is positive in case of the type 3 wave.

In addition, the operator $L^1(\varepsilon; 1 - \varepsilon\tilde{\gamma})$ and $L^3(\varepsilon; 1 - \varepsilon\tilde{\gamma})$ have the same high-frequency eigenvalue Λ_2 (up to order ε^2). \square

The proofs of lemmas 5.2 and 5.4 show the presence of a high-frequency eigenvalue for a semi-kink in case the bias current is not small. In the following we will show that the eigenvalue appears when the bias current is larger than $\sqrt{\varepsilon} + \mathcal{O}(\varepsilon)$.

Because we do not have an analytic expression for the type 2 and type 3 semi-kink in the small forcing limit, the analysis is done only for the type 1 semi-kink.

LEMMA 5.5. *There is a critical value γ_{hf} , $\gamma_{\text{hf}} = \sqrt{\varepsilon} + \mathcal{O}(\varepsilon)$ such that for all $\gamma \in (\gamma_{\text{hf}}, \gamma_{\text{cr}})$ the operator $L^1(\varepsilon; \hat{\gamma})$ has a high frequency eigenvalue that up to $\mathcal{O}(\varepsilon^3)$ is attached to the lowest boundary of the continuous spectrum. The corresponding eigenvector is localized and changes sign between any two adjacent sites.*

The appearance of this eigenvalue and the structure of its eigenvector is checked numerically in section 6.

Proof. Again, we write for an eigenvector

$$v_n = \begin{cases} cl^{-n}, & n \leq 0, \\ \hat{c}cl^{n-1}, & n \geq 1, \end{cases}$$

for some c , \hat{c} and $|\ell| < 1$ and we substitute this in the eigenvalue problem. We first consider $\gamma = \sqrt{\varepsilon}\hat{\gamma}$. This gives $A_n = 1 - \frac{\varepsilon\hat{\gamma}^2}{2} - \frac{\varepsilon^2\hat{\gamma}^4}{8} + \mathcal{O}(\varepsilon^{5/2})$, if $n \neq 0, 1$, $A_0 = 1 - \frac{\varepsilon\hat{\gamma}^2}{2} - \varepsilon^{3/2}\pi\hat{\gamma} - \varepsilon^2(\frac{\hat{\gamma}^4}{8} + \frac{\pi^2}{2}) + \mathcal{O}(\varepsilon^{5/2})$ and $A_1 = 1 - \frac{\varepsilon\hat{\gamma}^2}{2} + \varepsilon^{3/2}\pi\hat{\gamma} - \varepsilon^2(\frac{\hat{\gamma}^4}{8} + \frac{\pi^2}{2}) + \mathcal{O}(\varepsilon^{5/2})$.

Using the same procedures, this implies $\hat{c}_{\pm} = -\sqrt{\varepsilon}\pi\hat{\gamma} - \varepsilon^{3/2}\hat{\gamma}^3\pi \pm \sqrt{\pi^2\hat{\gamma}^2\varepsilon + 2\pi^2\hat{\gamma}^4\varepsilon^2 + 1}$ and

$$\frac{1}{\ell_{\pm}} = \varepsilon\pi^2 \pm 2\sqrt{\pi^2\hat{\gamma}^2\varepsilon + 2\pi^2\hat{\gamma}^4\varepsilon^2 + 1} = \pm 1 + \frac{\varepsilon\pi^2(1 \pm \hat{\gamma}^2)}{2} + \mathcal{O}(\varepsilon^2).$$

For $\hat{\gamma} > 1$ there are two solutions $|\ell_{\pm}| < 1$; $\ell_+ > 0$ corresponds to the largest eigenvalue and also exists for $\hat{\gamma} \leq 1$ (Lemma 5.2); $\ell_- < 0$, so that its associated eigenvector v_n indeed changes sign between any two adjacent sites.

The value $\gamma_{\text{hf}} = \sqrt{\varepsilon} + \mathcal{O}(\varepsilon)$ indicates the appearance of this high frequency eigenvalue from the continuous spectrum. It follows from a straightforward analysis that this eigenvalue exists, i.e. $\ell_- \in (-1, 0)$ exists, for all $\gamma \in (\gamma_{\text{hf}}, \gamma_{\text{cr}})$, and the corresponding eigenvalue is $\Lambda_- = -1 + (\frac{\hat{\gamma}^2}{2} - 4)\varepsilon + \hat{\gamma}^4/8\varepsilon^2 + \mathcal{O}(\varepsilon^3)$. Up to $\mathcal{O}(\varepsilon^3)$ this eigenvalue is nothing else but the lower boundary of the continuous spectrum. \square

6. Numerical computations of the discrete system. To accompany our analytical results, we have used numerical calculations. For that purpose, we have made a continuation program based on Newton iteration technique to obtain the stationary kink equilibria of (2.3) and (2.4) and an eigenvalue problem solver in MATLAB. To start the iteration, one can choose either the continuum solutions discussed in section 3, i.e., the case where the lattice spacing parameter $a = 0$, or trace the equilibria from the uncoupled limit $\varepsilon = 0$ ($a \rightarrow \infty$) as discussed in the previous section. We use the number of computational sites $2N = 800$ for parameter values of $a = 0.05$ or larger ($\varepsilon = 20$ or lower).

6.1. Stability of type 1 lattice semifluxon. The type 1 lattice semifluxon $\Phi_\pi^1(n; \varepsilon; 0)$, $n \in \mathbb{Z}$ has been studied analytically both in the strong coupling limit ($a \ll 1$, or $\varepsilon \gg 1$) and the weak coupling limit ($a \gg 1$, $\varepsilon \ll 1$). In Figure 6.1(a), $\Phi_\pi^1(n; \varepsilon; 0)$ is plotted for two different values of the coupling parameter ε . For a given value of ε , one can use as initial guess in the numerical procedure either a solution from the continuous limit (3.10) or from the uncoupled limit that has been discussed in the preceding sections.

In Figure 6.1(b), we present the numerically calculated spectrum of the type 1 semifluxon with $\gamma = 0$ as a function of the lattice spacing parameter. The approximate largest eigenvalue (4.9), derived for a small, and the one derived in Lemma 5.2 for a large, are in a good agreement with the numerically obtained largest eigenvalue. Any eigenvalue below $\Lambda = -1$ belongs to the continuous spectrum. For a close to zero we do not see dense spectra because of the number of sites we used. By increasing the sites-number we will obtain a more dense spectrum.

There is only one eigenvalue outside the phonon bands, the largest eigenvalue as studied in Lemma 5.2. This is in contrast to the case of an ordinary lattice 2π -kink [17, 19] where there is an internal mode bifurcating from the phonon band when the parameter a increases.

If Fig. 6.1(b) shows the spectrum of the type 1 semifluxon as a function of the coupling parameter ε ($\varepsilon = 1/a^2$) for a fixed bias current γ , in Fig. 6.2 we present the numerically calculated spectrum of the type 1 lattice semifluxon as a function of γ for a fixed ε , $\varepsilon = 0.25$.

Lemmas 5.2 and 5.5 established the existence of two eigenvalues (for ε small enough) for the stability problem associated to the type 1 semifluxon, the largest eigenvalue and an additional eigenvalue which bifurcates from the lower edge of the phonon band for bias current $\gamma > \gamma_{\text{hf}}$. It follows from the numerical simulations that these are indeed the only two eigenvalues (Figure 6.2). For $\varepsilon = 0.25$, this minimum bias current γ_{hf} is approximately 0.466. Interestingly, according to Lemma 5.5 the bifurcation appears at $\gamma_{\text{hf}} = \sqrt{\varepsilon} = 0.5$ at leading order in ε . This is in remarkably good agreement with the numerical result, especially since the error is $\mathcal{O}(\varepsilon)$ and $\varepsilon = 0.25$.

To picture the appearance of the high-frequency eigenvalue, all eigenvalues for the truncated $2N \times 2N$ -matrix associated with $L^1(\varepsilon; \gamma)$ are determined and the eigenvectors of the two largest eigenvalues and the two smallest eigenvalues are presented in Figures 6.3-6.5 for various values of γ and a fixed ε . It can be observed that there is

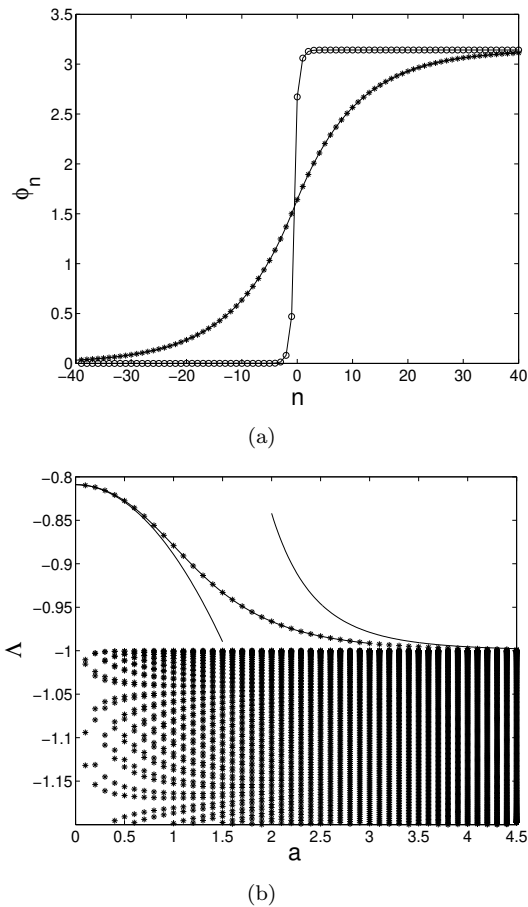


FIG. 6.1. (a) Two lattice semifluxons of type 1 with no bias current ($\gamma = 0$) are plotted as a function of the lattice index, namely the kink for strong coupling with $\varepsilon = 100$ (equivalently, a very small lattice spacing $a = 0.1$) ($- * -$), i.e. close to (3.10) and the kink for weak coupling with $\varepsilon = \frac{1}{4}$ (equivalently, a large lattice spacing $a = 2$) ($- o -$). (b) Numerically computed spectrum of a lattice semifluxon against the lattice spacing parameter a with $\gamma = 0$. We used the number of sites $2N = 300$. We zoom in the plot of spectra around -1 for clarity. The bold-solid-line is the calculated approximate function for the point spectrum using perturbation theory for a small resp. for ε small.

always a localized eigenfunction associated with the largest eigenvalue. In Figure 6.3 ($\gamma = 0$), none of the other eigenvectors can be associated with localized eigenfunctions and in Figures 6.4 and 6.5, the birth of the localized eigenfunction associated with the smallest eigenvalue can be observed.

If we keep increasing γ further, then there is a critical applied bias current at which the largest eigenvalue becomes 0. Numerical computations show that this critical value is $\gamma_{\text{cr}}(\varepsilon)$ above which static lattice semifluxons disappear.

The critical bias current for the existence of a static type 1 lattice semifluxon in the continuum limit and for a very weak coupling in the discrete system has been discussed and analytical expressions were given in sections 3, 4 and 5, respectively. In Figure 6.6, the numerically calculated critical bias current γ_{cr} of the discrete system (2.3) as a function of the lattice spacing a is presented. The approximate functions, given in (4.2) for small a , and in (5.4) for large a (small ε) are presented as dashed lines.

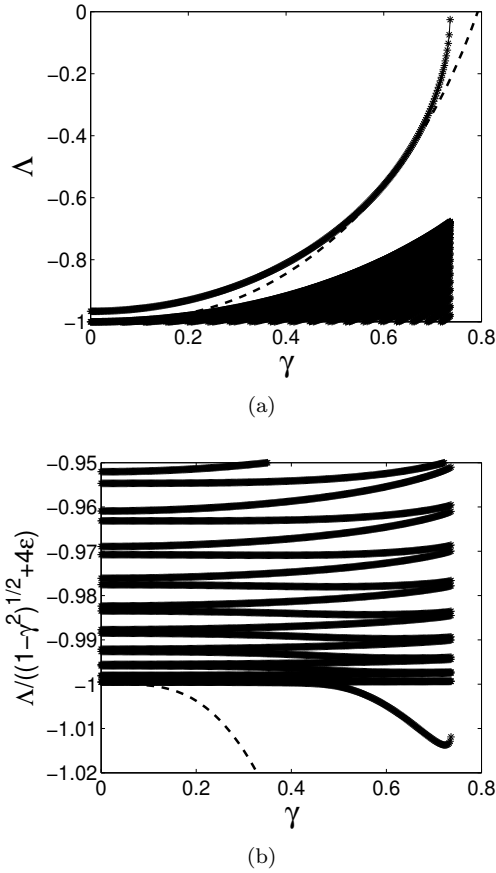


FIG. 6.2. (a) Spectrum of the type 1 semifluxon as a function of the applied bias current γ for a value of the coupling constant $\epsilon = 0.25$. The dashed line is theoretical prediction from (5.13). In (b) we zoom in on the spectrum around -1 for clarity. The spectrum is normalized to the lower edge of the phonon band, i.e. $\sqrt{1 - \gamma^2} + 4\epsilon$, such that the appearance of a high frequency eigenvalue can be seen clearly.

6.2. Instability of type 2 lattice semifluxon. In the continuum models we have seen that for γ small, the instability of the type 2 semikink is mainly determined by the instability of the 3π -kink in the continuum models for $\gamma = 0$. So we start this section by looking at the stability of the 3π -kink in the discrete model. We will denote the 3π -kink by $\Phi_{3\pi}^2(n; \epsilon; 0)$, where as before the coupling parameter ϵ and the lattice spacing a are related by $\epsilon = \frac{1}{a^2}$.

Using our continuation program, we have followed a 3π -kink solution from the continuous limit $0 < a \ll 1$ up to the uncoupled situation $\epsilon = 0$ (i.e., $a = \infty$). We obtain that $\Phi_{3\pi}^2(n; 0; 0)$ is given by

$$(6.1) \quad \Phi_{3\pi}^2(n; 0; 0) = \begin{cases} 0, & n = -1, -2, \dots \\ 2\pi, & n = 0, \\ \pi, & n = 1, \\ 3\pi, & n = 2, 3, \dots \end{cases}$$

Note that this discrete configuration is not monotonically increasing as opposed to

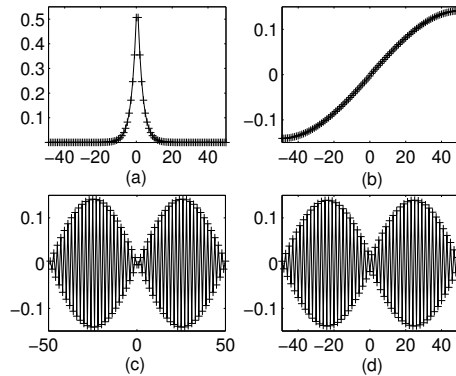


FIG. 6.3. The eigenvectors associated the two largest eigenvalues and the two smallest eigenvalues of the truncated $2N \times 2N$ -matrix associated with $L^1(\varepsilon; \gamma)$ (the type 1 discrete semikink) for $\varepsilon = 0.25$ and $\gamma = 0$. The results are shown with $2N = 100$ for clarity. Shown are the eigenvector of (a) the largest eigenvalue, (b) the second one, (c)-(d) the last two eigenvalues. There is only one eigenvalue for $L^1(\varepsilon; \gamma)$ as there is only one localized eigenvector.

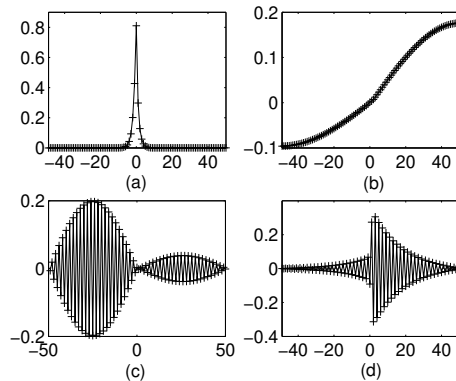


FIG. 6.4. The same as Fig. 6.3 for $\gamma = 0.5$.

the continuum configuration, which is monotonic.

In Figure 6.7, we present the numerically obtained eigenvalues of a 3π -kink as a function of the lattice spacing a . For small a , the largest eigenvalue is indeed increasing as is predicted by the perturbation theory (4.10). As soon as the lattice spacing is of order one, the largest eigenvalue decreases and becomes zero at approximately $a = 1.7521$.

After establishing that increasing the lattice spacing can stabilize the 3π -kink at $\gamma = 0$, we continue by looking at the stability of the 2π -kink for $\gamma > 0$. Interestingly, increasing the lattice spacing does not stabilize a type 2 semikink for $\gamma > 0$. In Figure 6.8, we show a plot of the type 2 semikinks for two values of ε as well as a plot of the largest eigenvalue as a function of ε for two particular values of γ , namely $\gamma = 0.01$ and $\gamma = 0.1$. We present the largest eigenvalue as a function of the coupling ε instead of the lattice spacing a as the eigenvalue changes most for small coupling (large lattice spacing). From Figure 6.8 it follows that the solutions are unstable even in the weak-coupling limit. This is interesting as in the limit for $\gamma \rightarrow 0$, the type 2 semikink

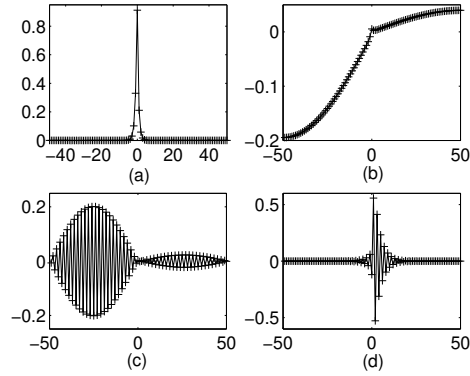


FIG. 6.5. The same as Figure 6.3 for $\gamma = 0.7$. Note that there are now two localized eigenvectors shown in (a) and (d). The smallest eigenvalue associated with (d) is -1.7357 while the lower edge of the phonon band is -1.7141 . Note also that neighboring sites of the eigenvector in (d) move out of phase indicating a high-frequency mode, contrary to the semikink's low-frequency mode in (a).

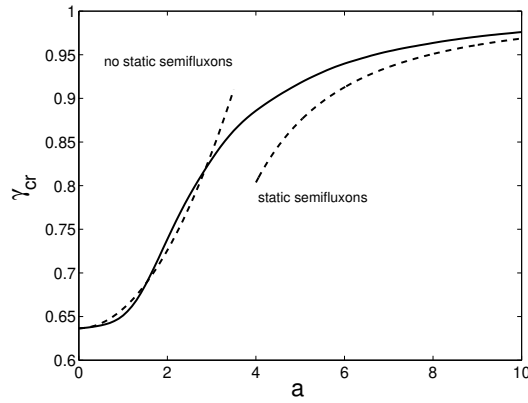


FIG. 6.6. The critical bias current of a static π -kink as a function of the lattice spacing parameter a . For γ above the critical current there is no static π -kink solution. The solid line is numerically obtained curve. Dashed lines are the theoretical predictions (4.2) for $a \ll 1$ resp. (5.4) for $a \gg 1$ ($\varepsilon \ll 1$).

can be seen as a concatenation of a 3π -kink and a -2π -kink. Both the 3π -kink and -2π -kink are stable for the coupling ε sufficiently small, while the type 2 semikink turns out to be unstable.

This instability issue can be explained by looking at the expression of a type 2 semikink when it is uncoupled ($\varepsilon = 0$). For the two particular choices of γ above, we get from the simulations that the configurations of these semi-kinks are given by

$$(6.2) \quad \Phi_{\pi}^2(n; 0; 0.01) = \begin{cases} 0 + \arcsin(0.01), & n \leq -1, \\ \pi - \arcsin(0.01), & n = 0, \\ \pi + \arcsin(0.01), & n = 1, \\ 3\pi + \arcsin(0.01), & 2 \leq n \leq 8, \\ 2\pi - \arcsin(0.01), & n = 9, \\ \pi + \arcsin(0.01), & n \geq 10, \end{cases}$$

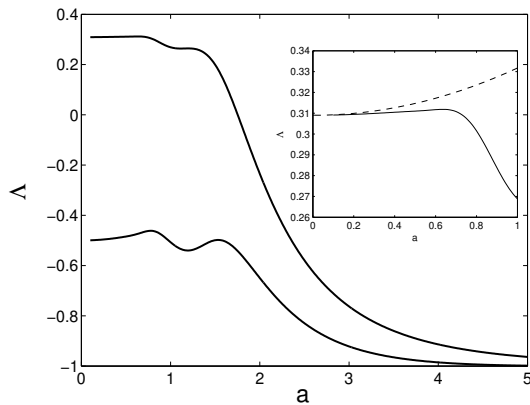


FIG. 6.7. Plot of the eigenvalues of a 3π -kink as a function of the lattice spacing parameter a . We zoom in the region with $a \ll 1$ where it shows that turning the lattice spacing on destabilizes the kink. The dashed line depicts the analytically computed approximation (4.10) to the largest eigenvalue of the 3π -kink.

and

$$(6.3) \quad \Phi_{\pi}^2(n; 0; 0.1) = \begin{cases} 0 + \arcsin(0.1), & n \leq -1, \\ \pi - \arcsin(0.1), & n = 0, \\ \pi + \arcsin(0.1), & n = 1, \\ 3\pi + \arcsin(0.1), & 2 \leq n \leq 6, \\ 2\pi - \arcsin(0.1), & n = 7, \\ \pi + \arcsin(0.1), & n \geq 8. \end{cases}$$

We see that there are two sites, namely $n = 0$ and $n = 9$ for $\gamma = 0.01$ and $n = 0$ and $n = 7$ for $\gamma = 0.1$, where Φ takes the value of an unstable fixed point of the discrete system (2.3). Looking only at sites numbered $n = 2$ to $n \rightarrow \infty$, $\Phi_{\pi}^2(n; 0; \gamma)$ can be viewed as a -2π lattice kink sitting on a site which is known to be unstable. If we look only at sites numbered $n = 6$ to $n \rightarrow -\infty$, $\Phi_{\pi}^2(n; 0; \gamma)$ can be seen as a deformed 3π lattice kink (at site $n = 0$, the phase Φ takes the value π instead of the value 2π as in the 3π -kink). Hence, it seems that coupling between the two kinks due to the presence of a nonzero γ is responsible for the instability.

It has been discussed in the previous sections that there is a critical bias current γ^* for the existence of a type 2 lattice semikink in the continuum models. However, we did not numerically calculate the critical bias current $\gamma^*(a)$ for discrete system (2.3).

6.3. Instability of type 3 lattice semifluxon. In this section, we will consider the type 3 semikinks, which will be denoted by $\Phi_{\pi}^3(n; \varepsilon; \gamma)$. In Lemmas 3.9 and 4.7 it has been shown that these kinks are unstable in the continuum models for small or zero lattice spacing.

The largest eigenvalue of a lattice type 3 semifluxon for three particular values of γ , i.e. $\gamma = 0.01, 0.1, 0.55$, is presented in Figure 6.9. Even though in the limit for $\gamma \rightarrow 0$, a semifluxon of this type is a concatenation of a 2π -kink and a $-\pi$ -kink which both can be stable in the discrete system, the type 3 semikink is unstable for all parameter values from the zero lattice spacing limit all the way to the zero coupling one. The explanation is similar to the one for a type 2 semikink discussed above.

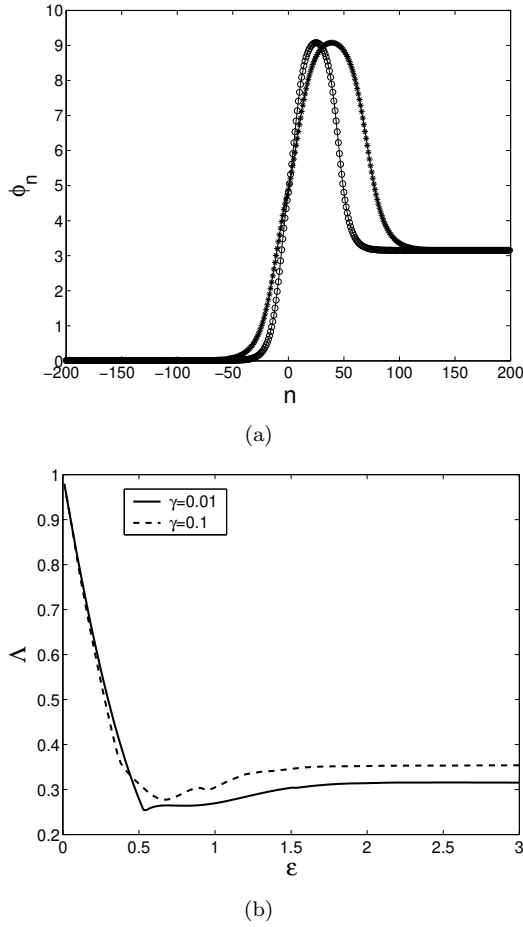


FIG. 6.8. (a) Plot of a type 2 semikink with $\gamma = 0.01$ for $\varepsilon = 100$ ($- * -$) and $\varepsilon = 40$ ($- o -$). (b) Plot of the largest eigenvalue of a type 2 semikink as a function of the coupling parameter ε . When $\varepsilon = 0$, the eigenvalue converges to $\Lambda = \sqrt{1 - \gamma^2}$.

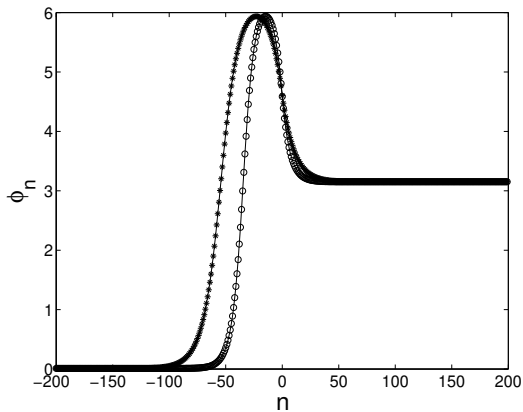
Indeed, for the three particular choices of γ above, $\Phi_\pi^3(n; 0; \gamma)$ is given by

$$(6.4) \quad \Phi_\pi^3(n; 0; 0.01) = \begin{cases} 0 + \arcsin(0.01), & n = -1, -2, \dots \\ \pi - \arcsin(0.01), & n = -6, \\ 2\pi + \arcsin(0.01), & n = -5, \dots, 0, \\ \pi + \arcsin(0.01), & n = 1, 2, \dots, \end{cases}$$

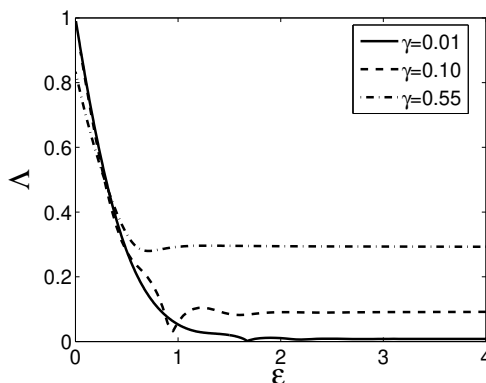
$$(6.5) \quad \Phi_\pi^3(n; 0; 0.1) = \begin{cases} 0 + \arcsin(0.1), & n = -1, -2, \dots \\ \pi - \arcsin(0.1), & n = -2, \\ 2\pi + \arcsin(0.1), & n = -1, 0, \\ \pi + \arcsin(0.1), & n = 1, 2, \dots, \end{cases}$$

and

$$(6.6) \quad \Phi_\pi^3(n; 0; 0.55) = \begin{cases} 0 + \arcsin(0.55), & n = -1, -2, \dots \\ \pi - \arcsin(0.55), & n = 0, \\ \pi + \arcsin(0.55), & n = 1, 2, \dots \end{cases}$$



(a)



(b)

FIG. 6.9. (a) Plot of a type 3 semikink with $\gamma = 0.01$ for $\epsilon = 100$ ($- * -$) and $\epsilon = 40$ ($- o -$). (b) Plot of the largest eigenvalue of a type 3 semikink as a function of the coupling parameter ϵ . When $\epsilon = 0$, the eigenvalue converges to $\Lambda = \sqrt{1 - \gamma^2}$.

One interesting point to note for the type 3 semikink is that the number of sites with value 2π is decreasing as γ increases. Starting from the continuum approximation of a type 3 semikink as the initial guess for the continuation program, the 2π -plateau disappears for $\gamma \geq \gamma^*(a)$ (see (4.1)). For $\gamma > \gamma^*$ the configuration at $\epsilon = 0$ is similar to the stable type 1 π -kink (5.2), apart from the value of the phase at the site with $n = 0$ (where the phase takes the value of an unstable fixed point).

Because analytical calculation of the spectrum of the type 3 semikink has been obtained in the small coupling limit and bias current close to 1 (Eqs. (5.17)), it is worth comparing the analytical predictions with numerical computations. The theoretical calculations shows that for ϵ small and γ close to 1, the type 3 semikink has at least two eigenvalues, one of which corresponds to a high frequency mode and the other to a positive eigenvalue.

Using the continuation of (6.6) for $\epsilon = 0.25$, the spectrum of the type 3 lattice semikink is presented in Figure 6.10 as a function of the applied bias current γ . Our numerics show that when γ is very close to γ_{cr} , the type 3 semikink has three eigenvalues, one of which corresponds to a high frequency mode and is below the

phonon band, while the other two are above the phonon band. The birth of this high-frequency mode is shown in Figure 6.10(c) and is qualitatively similar to the case of the type 1 lattice semikink. The two eigenvalues which exist for all values of γ can be observed in Figure 6.10(a) and (b).

7. Conclusions. We have performed an existence and stability analysis for three types of lattice π -kink solutions of the discrete $0-\pi$ sine-Gordon equation and its continuum limits. Analytical results have been established in the continuum limits and in the weak-coupling case. It has been shown that in the continuous $0-\pi$ sine-Gordon equation, π -kinks of type 1 are stable and the other types are unstable. The introduction of discreteness destabilizes the unstable π -kinks even more. An approximation to the largest eigenvalue of all types of π -kinks has been derived both in the continuum and the weak coupling limits.

For future research, it is of interest to study the nucleation of kinks and antikinks when a constant force, or bias current, γ that is above the critical value γ_{cr} is applied – see Figure 3.2(b). One question that can be addressed is the mechanism and the frequency of the nucleation as a function of the applied constant force, especially in the presence of a damping coefficient (which has not been considered in this paper). In work in progress, the stability of the type 3 semifluxons in the presence of defects is studied. These semifluxons are unstable, but the largest eigenvalue is close to zero. In fact, a type 3 semifluxon consists of a fluxon and a semifluxon with the opposite polarity. In experiments, the presence of a fluxon nearby a semifluxon can influence a junction measurement [12]. Because a fluxon can be pinned by a defect [18], one can expect to have a stable type 3 semifluxon when there is a defect present in the system.

Acknowledgments. H.S. wishes to thank Panayotis Kevrekidis for numerous useful interactions and discussions.

REFERENCES

- [1] F. V. Atkinson, *Discrete and Continuous Boundary Problems*, vol. 8 of Mathematics in Science and Engineering, (Academic Press, New York, 1964).
- [2] C. Baensens, S. Kim, and R. S. MacKay, *Localised modes on localised equilibria*, *Physica D* **113** (1998), pp. 242–247
- [3] N. J. Balmforth, R. V. Craster, and P. G. Kevrekidis, *Being stable and discrete*, *Physica D* **135** (2000), pp. 212–232.
- [4] J.J.A. Baselmans, A.F. Morpurgo, B.J. van Wees, and T.M. Klapwijk, *Reversing the direction of the supercurrent in a controllable Josephson junction*, *Nature* **397** (1999), pp. 43–45.
- [5] O. M. Braun and Yu. S. Kivshar, *Nonlinear dynamics of the Frenkel-Kontorova model*, *Phys. Rep.* **306** (1998), pp. 1–108.
- [6] O. M. Braun, Yu. S. Kivshar, and M. Peyrard, *Kink's internal modes in the Frenkel-Kontorova model*, *Phys. Rev. E* **56** (1997), pp. 6050–6064.
- [7] L.N. Bulaevskii, V.V. Kuzii, and A. A. Sobyenin, *Superconducting system with weak coupling to the current in the ground state*, *JETP Lett.* **25** (1977), pp. 290–294; L.N. Bulaevskii, V.V. Kuzii, A. A. Sobyenin, and P.N. Lebedev, *On possibility of the spontaneous magnetic flux in a Josephson junction containing magnetic impurities*, *Solid State Comm.* **25** (1978), pp. 1053–1057.
- [8] A. Champneys and Yu. S. Kivshar, *Origin of multikinks in dispersive nonlinear systems*, *Phys. Rev. E* **61** (2000), pp. 2551–2554.
- [9] B. V. Chirikov, *A Universal Instability of Many-Dimensional Oscillator Systems*, *Phys. Rep.* **52** (1979), pp. 264–379.
- [10] G. Derks, A. Doelman, S. A. van Gils and T. P. P. Visser, *Travelling waves in a singularly perturbed sine-Gordon equation*, *Physica D* **180** (2003), pp. 40–70.
- [11] J. Guckenheimer and P. Holmes, *Nonlinear Oscillations, Dynamical Systems and Bifurcation of Vector Fields*, 2nd ed. (Springer-Verlag, New York, 1986).

- [12] D. J. van Harlingen, *Phase-sensitive tests of the symmetry of the pairing state in the high-temperature superconductors—Evidence for $d_{x^2-y^2}$ symmetry*, Rev. Mod. Phys. **67** (1995), pp. 515–535.
- [13] D. Henry, *Geometry Theory of Semilinear Parabolic Equations*, Vol. 840 of *Lecture notes in mathematics* (Springer-Verlag, 1981).
- [14] H. Hilgenkamp, Ariando, H. J. H. Smilde, D.H.A. Blank, G. Rijnders, H. Rogalla, J.R. Kirtley, and C.C. Tsuei, *Ordering and manipulation of the magnetic moments in large-scale superconducting π -loop arrays*, Nature **422** (2003), pp. 50–53.
- [15] T.Kato, *Perturbation Theory of Linear Operators* (Springer, 1976).
- [16] T. Kato and M. Imada, *Vortices and Quantum tunneling in Current-Biased $0-\pi-0$ Josephson Junctions of d -wave Superconductors*, J. Phys. Soc. Jpn. **66** (1997), pp. 1445–1449.
- [17] P. G. Kevrekidis and C. K. R. T. Jones, *Bifurcation of internal solitary wave modes from the essential spectrum*, Phys. Rev. E **61** (2000), pp. 3114–3121.
- [18] Yu. S. Kivshar and B. A. Malomed, *Dynamics of solitons in nearly integrable systems*, Rev. Mod. Phys. **61** (1989), pp. 763–915; *ibid.* **63** (1991), pp. 211 (Addendum).
- [19] Yu. S. Kivshar, D. E. Pelinovsky, T. Cretegny, and M. Peyrard, *Internal Modes of Solitary Waves*, Phys. Rev. Lett. **80** (1998), pp. 5032–5035.
- [20] A. B. Kuklov, V.S. Boyko, and J. Malinsky, *Instability in the current-biased $0-\pi$ Josephson junction*, Phys. Rev. B **51** (1995), pp. 11965–11968; *ibid.* **55** (1997), pp. 11878 (Erratum).
- [21] R. S. MacKay and J. A. Sepulchre, *Multistability in networks of weakly coupled bistable units*, Physica D **82** (1995), pp. 243–254.
- [22] E. Mann, *Systematic perturbation theory for sine-Gordon solitons without use of inverse scattering methods*, J. Phys. A: Math. Gen. **30** (1997), pp. 1227–1241.
- [23] Y. Nomura, Y. H. Ichikawa, and A. T. Filippov, *Stochasticity in the Josephson Map*, J. Plasma Phys. **56** (1996), pp. 493–506.
- [24] D. E. Pelinovsky, P. G. Kevrekidis, and D. J. Frantzeskakis, *Stability of discrete solitons in nonlinear Schrödinger lattices*, Physica D **212** (2005), pp. 1–19.
- [25] M. Peyrard and M. D. Kruskal, *Kink dynamics in the highly discrete sine-Gordon system*, Physica D **14** (1984), pp. 88–102.
- [26] M. Peyrard and M. Remoissenet, *Solitonlike excitations in a one-dimensional atomic chain with a nonlinear deformable substrate potential*, Phys. Rev. B **26** (1982), pp. 2886–2899.
- [27] N. R. Quintero, A. Sanchez, and F. G. Mertens, *Anomalous Resonance Phenomena of Solitary Waves with Internal Modes*, Phys. Rev. Lett. **84** (2000), pp. 871–874.
- [28] P. Rosenau, *Hamiltonian dynamics of dense chains and lattices: or how to correct the continuum*, Phys. Lett. A **311** (2003), pp. 39–52.
- [29] V.V. Ryazanov, V.A. Oboznov, A.Yu. Rusanov, A.V. Veretennikov, A.A. Golubov, and J. Aarts, *Coupling of Two Superconductors through a Ferromagnet: Evidence for a π Junction*, Phys. Rev Lett. **86** (2001), pp. 2427–2430.
- [30] A. Scott, *Nonlinear science: emergence and dynamics of coherent structures*, Oxford University Press, 1999.
- [31] H. Susanto and S. A. van Gils, *Instability of a lattice semifluxon in a current-biased $0-\pi$ array of Josephson junctions*, Phys. Rev. B **69** (2004), pp. 092507–092510.
- [32] H. Susanto, S. A. van Gils, T. P. P. Visser, Ariando, H. J. H. Smilde, and H. Hilgenkamp, *Static semifluxons in a long Josephson junction with π -discontinuity points*, Phys. Rev. B. **68** (2003), pp. 104501–104508.
- [33] E.C. Titchmarsh, *Eigenfunction expansions associated with second-order differential equations* (2nd edition), Oxford University Press, 1962.
- [34] C.C. Tsuei and J.R. Kirtley, *Pairing symmetry in cuprate superconductors*, Rev. Mod. Phys. **72** (2000), pp. 969–1016.
- [35] O. Vávra, S. Gaži, D. S. Golubović, I. Vávra, J. Dérer, J. Verbeeck, G. Van Tendeloo, and V. V. Moshchalkov, *The 0 and the π phase Josephson coupling through an insulating barrier with magnetic impurities*, Phys. Rev. B **74** (2006), pp. 020502–020505.
- [36] K. Yosida, *Functional Analysis* (Springer, 1995).

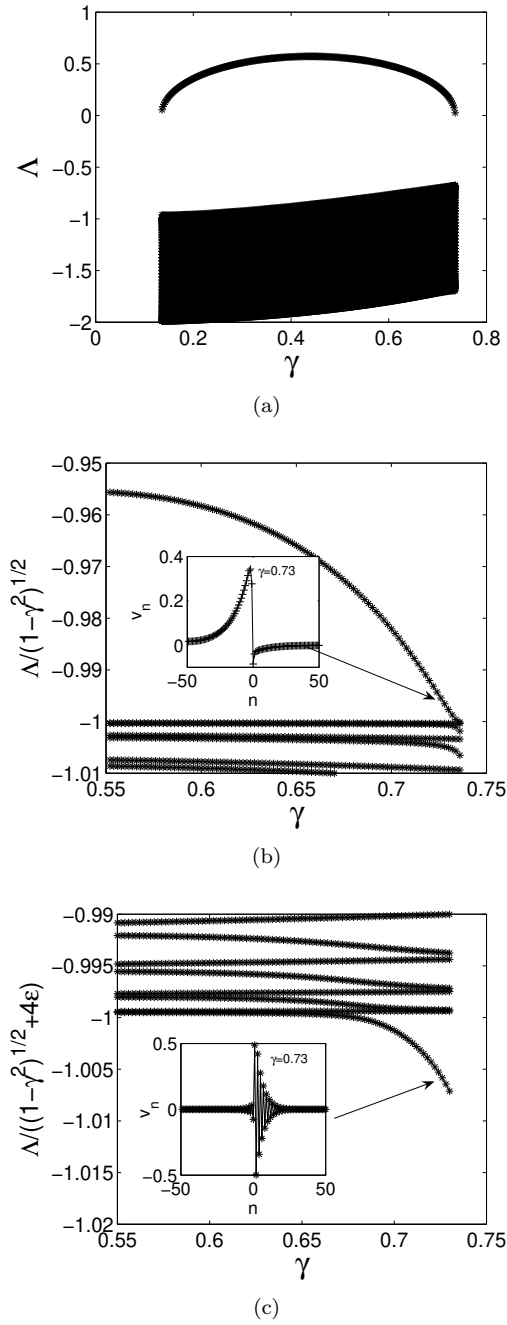


FIG. 6.10. Spectrum of the type 3 semifluxon as a function of the applied bias current γ for a value of the coupling constant $\varepsilon = 0.25$. In (b) and (c) we zoom in near the phonon band for clarity. In (b), the spectrum is normalized to the upper edge of the phonon band, i.e. $\sqrt{1-\gamma^2}$ and in (c) it is normalized to the lower edge of the phonon band, i.e. $\sqrt{1-\gamma^2} + 4\varepsilon$. The disappearance of a high-frequency mode in the lower edge of the phonon band can be clearly observed in (c). The insets in (b) and (c) show the eigenfunctions of the two eigenvalues just above resp. just below the phonon band for $\gamma = 0.73$.